Fabrication of Photosystem I Protein Films with Improved Stability

By

Siyuan Yang

Thesis

Submitted to the Faculty of the

Graduate School of Vanderbilt University

in partial fulfillment of the requirements

for the degree of

MASTER OF SCIENCE

in

Chemical Engineering

May, 2015

Nashville, Tennessee

Approved:

Kane Jennings, Ph.D.

David Cliffel, Ph.D.

To the Jennings Group, past present and future

and

To my beloved family, infinitely supportive

ACKNOWLEDGEMENTS

First of all, I would like to acknowledge and thank Prof. Kane Jennings for devoting all his attention to direction in research. He always encouraged me and gave me enough understanding while having high expectations. He helped me develop a professional research practice skills and allowed me to operate the research process in my own calendar. He provided me greater opportunities to practice the experimental skills, presentation skills and writing skills. Under his guidance, my skills developed a lot. I truly admire him and respect, not only his professional attainment and achievements, but also his kindness and genuine concern.

I would also like to acknowledge and thank Prof. David Cliffel, who introduced me to the electrochemical field. I would never forget my using for the electrical chemical station and his explanations for the data comparison among experiments.

In addition, I would like to thank Dr. Gabriel Leblanc, who was a graduate student in Prof. Cliffel's lab and currently works as post doctor fellow at University of Texas-Austin. He helped me a lot in the PSI project. He explained me the theory of PSI immobilized on the electrode in detail. And he showed me to measure and phototcurrent and over potential for the electrode hand by hand. Besides, he has organized the sub group meeting every two other week for a long time. He gave a consummate conclusion for our technique and results of the experiment and always gave us promising guidance for future experiment. Thanks to my past lab-mate, Escobar Carlos, Gunther Darlene, Max Robinson and Ian Njoroje. I enjoyed coming into lab everyday. Carlos performed the impedance experiments, he helped me a lot to overcome my difficulty when I come to the lab. I hope he can be a great scientist, as he always wanted to. Ian always organized the lab very well, he always found what we want for the experiment very

fast. Besides, most of time, Ian made gold-coated Si wafers in the lab. Max had many new ideas for the project, and he always shared his ideas with us to help us develop our design for the experiments.

I would also like to thank Ben for training me to operate profilometer, ellipsometer, Zetaslester and UV-vis in the VINSE. Dr. Dmitry taught me how to use FT-IR and QCM-D. Undergraduates Muhammad Zainuddin, James Mansfield and Helena Keller from Michigan Tech University helped me a lot in preparing experiments and doing tests. Thanks also to Prof. Brad for giving us opportunities to share and get new ideas.

Finally, I acknowledge my financial support from the department of Chemical and Biomoleculer Engineering, USDA 2013-67021-21029 and EPA SU-83528701.

TABLE OF CONTENTS

LIST OF TABLES

LIST OF FIGURES

Chapter 1

Introduction

Although fossil-based resources provide the vast majority of our energy currently, it is necessary to develop strategies for affordable alternative energy. Due to its huge capacity, solar energy can be an important alternative energy source to propel our society toward the future. On our planet, photosynthesis is the most important solar energy conversion process.[1] Plants, algae and cyanobacteria are able to convert the energy of sunlight into stored energy in the form of reduced carbon.[2] An integral membrane protein that drives photosynthesis in these systems is Photosystem I (PSI) (Figure 1), a 500kDa nanoscale protein complex that can convert solar energy into chemical energy with a quantum yield near unity.[3] Photons are absorbed by the chlorophylls distributed along the peripheral surface of PSI and transferred to a special pair of chlorophyll molecules known as the P_{700} reaction center, which excites an electron to a higher energy level in order to travel through an electron transfer chain to a terminal iron-sulfur acceptor (F_B) in about 10-30 ps.[4] By extracting PSI from a suitable source and assembling it as a thin film onto electrode substrates, this light-driven electron transfer process will drive electrons between the electrode and solution-phase mediator species with appropriate formal potentials,[5] utilizing PSI as the photoactive, electroactive conduit. Due to the rapid charge separation and high conversion efficiency of PSI, researchers around the world are actively investigating its incorporation into functional biohybrid devices.[6-10]

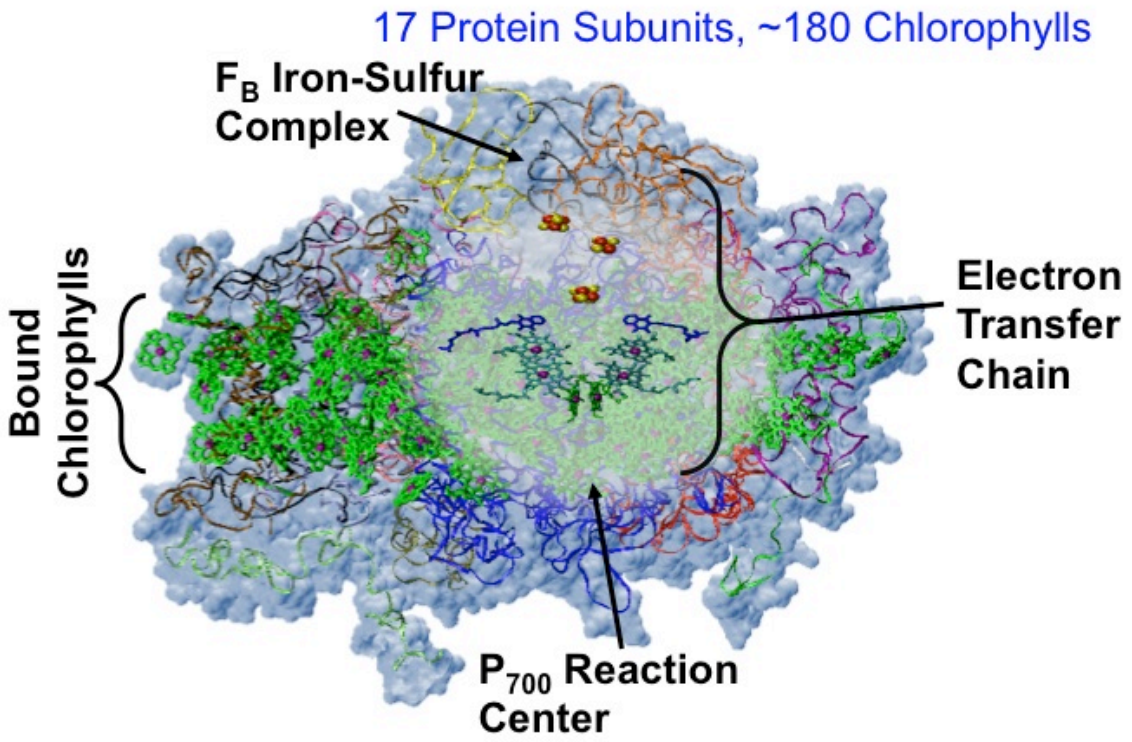

Figure 1. The structure of Photosystem I (PSI)[11]

Our group and others have made several key advances to integrate PSI with non-bio-biological systems for the design of more efficient biohybrid wet cells.[12-19] Frolov et al. fabricated a photoelectronic device by direct chemical binding of PSI to metal surfaces.[4] He also indicated that multilayer films of PSI, deposited monolayer by monolayer with Pt photodeposited at the acceptor site, increased photovoltages well beyond monolayer films of PSI. Mershin et al. has designed a low-cost PSI biophotovoltaic solar cell device by stabilizing dry PSI via surfactant peptides self-assembled on nanostructured semiconductors.[19] Our group has deposited PSI on a variety of substrates to increase photocurrent generation since 2004. Initially, our group deposited and studied monolayer PSI films deposited onto gold surfaces. Ciobanu et al. identified both P700 and F_A/F_B peaks of a PSI monolayer on a hydroxyl-terminated hexanethiolate SAM film using cyclic voltammetry and square wave voltammetry.[5] Faulkner et

al. developed a vacuum-assisted drop-casting method for covalent attachment of PSI onto an amine-terminated gold surface and generated ~80 fold improvements in photocurrent compared to previous tests.[20] Ciesielski et al. reported a method to assemble multilayer PSI films ranging from 0.4 – 3 μm, based on the number of drop-casting deposition steps, on a variety of substrates with controlled thickness (Figure 2).[21] We observed that thicker PSI films (multilayer) on electrode substrates resulted in significantly larger photocurrents since they increase light absorption and provide more sites where charge separation may occur.

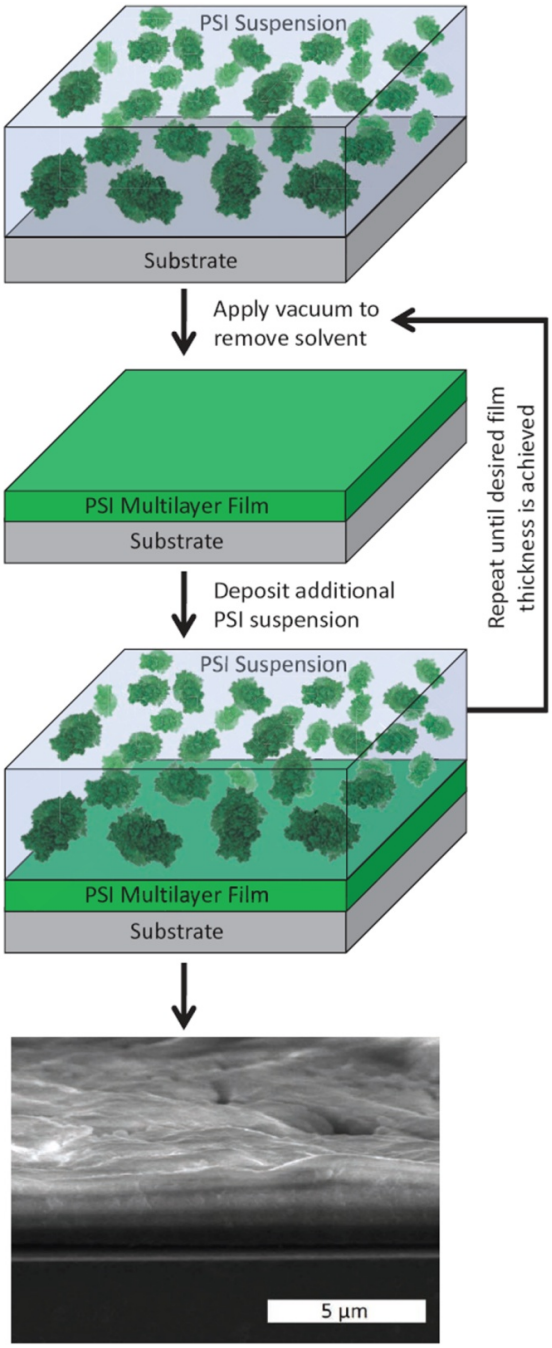

Figure 2. General procedure for the deposition of thick "multilayer" films of PSI. As depicted, the thickness of the resulting film can be adjusted by repeating the deposition process or by using different concentrations of PSI in the solution. The bottom panel shows an SEM image of the cross-section of the film following seven deposition steps. Image reproduced with permission from John Wiley and Sons. Image originally published by Ciesielski et al. in 2010[22]

In addition, LeBlanc et al. has immobilized PSI multilayer films onto p-Si electrodes and increased the photocurrent by 80-times more than that produced by similar multilayers on gold under identical conditions.[23]

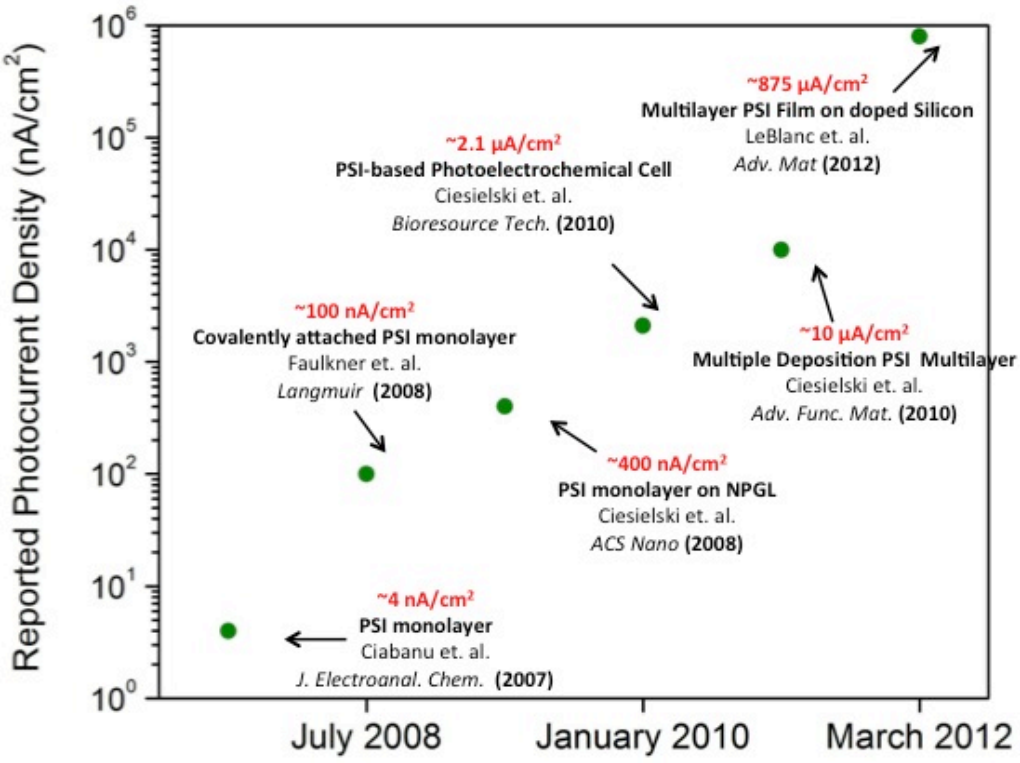

Figure 3. Photocurrent trend by the Jennings-Cliffel group from 2007 to 2012

Although we have shown that thicker PSI films can generate higher photocurrents, the stability of the current must be taken into consideration. Previously, Ciesielski et al. tested the stability of a prototype "wet" cell with PSI multilayer films over a period of 280 days by keeping the cell in the dark and testing it periodically in light (Figure 4). This approach was taken to investigate if PSI could remain functional over periods of time that extend well beyond the normal growing season of the source plant. However, the photocurrent reached its peak on the

second test day, decreased by 50% on the third test day, and then, the photocurrent remained stable for the remaining 9 months. The decrease in current from the second to the third day was attributed to some desorption and/or degradation of a fraction of PSI complexes that were not well stabilized when exposed in the mediator solution. As PSI is now being investigated in a broader array of solar conversion systems, including solid-state devices[24] and composite films[25], the methods to stabilize the protein complex within these systems could be highly important. Thus, here we seek to develop a method to stabilize PSI multilayer films on gold substrates.

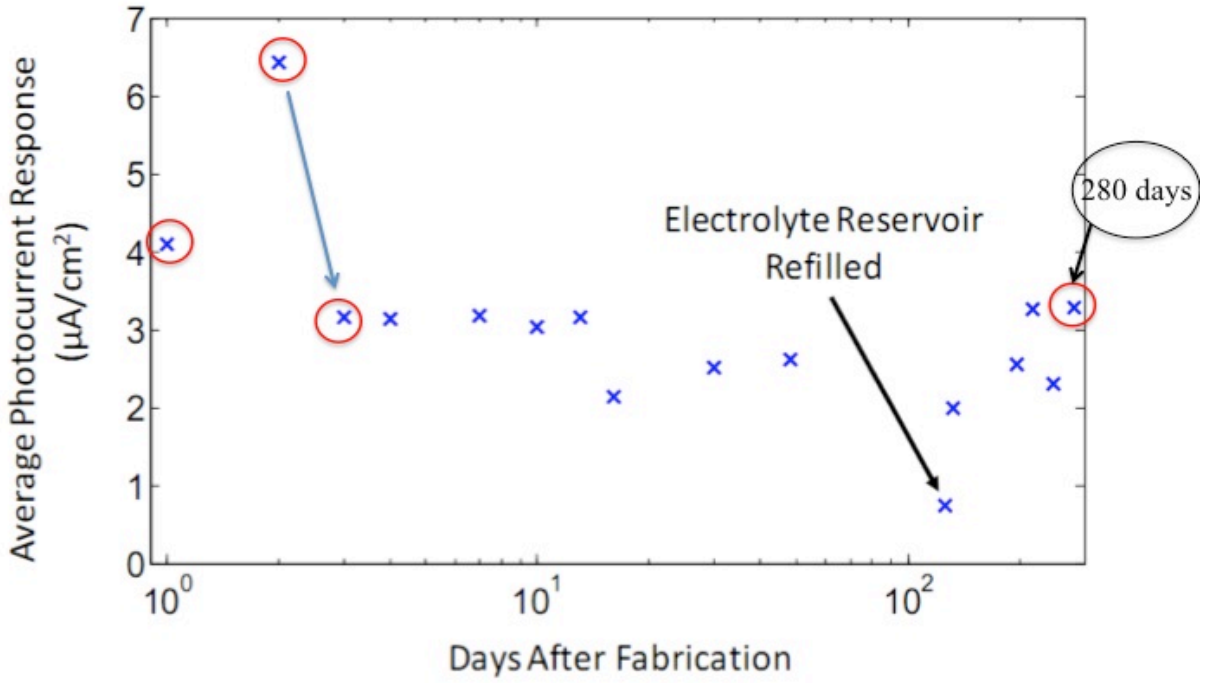

Figure 4. Stability of PSI Prototype Cell[16]

To make stable electrode systems based on PSI multilayer films, two objectives must be achieved. First, the thickness of PSI multilayer films should be stable. As will be shown here, when multilayer PSI films are exposed to aqueous solution, the thickness of PSI films exhibits a significant decrease due to desorption of PSI proteins from the films. Second, the electrode

interface should be stable. For example, since many non-noble metal electrodes such as silicon can oxidize to affect system performance, we have selected the stable and noble gold electrode as the substrate here, which allows us to directly focus on the stability of PSI as a film without the effects of electrode degradation.

To improve the stability of PSI films, we have investigated particular molecules to cross-link adjacent PSI proteins in multilayer PSI films on substrates. Cross-linking refers to the connecting of polymers or proteins via covalent bonds. In this work, covalent bonds were formed between two proteins to link the complexes by bio-functional reagents. Three cross-linkers, glutaraldehyde (GA), terephthalaldehyde (TPDA), and 2-iminothiolane (2IT) were used to stabilize PSI films on gold substrates. The thickness, topography, and electrochemical properties of PSI films were analyzed before and after exposure to aqueous buffer solutions to assess the performance of the different cross-linkers. The cross-linking reaction for the three molecules proceeded in the following two ways, based on the functionality of the cross-linker. First, an easy and effective way to cross-link is to generate imine covalent bonds, realized by reaction between aldehyde groups and amine groups in proteins under mild aqueous conditions. For TPDA and GA that exhibit terminal aldehyde groups on both sides, they convert and link amine groups on one protein to other amino termini nearby, [26, 27] generating imine groups (Eqn. 1, Eqn. 2).

Second, 2IT could similarly work with amines in the proteins to stabilize protein complexes via generated covalent bonds. When 2IT attaches to terminal amine groups, the sulfur-carbon bond is broken (Eqn. 3) to introduce a terminal thiol group. Adjacent thiol groups from two different proteins can react to form disulfide linkages to crosslink the proteins (Eqn.

4).[28] In other cases, 2IT-modified groups can react directly to proteins containing terminal thiol (cysteine) groups (Eqn. 5) to stabilize the proteins. [29, 30]

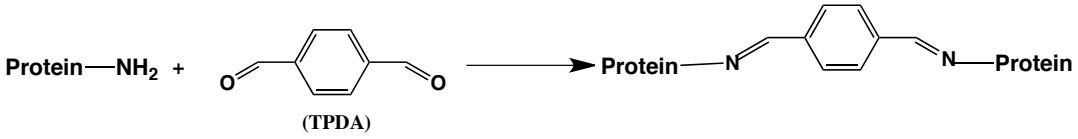

(1)

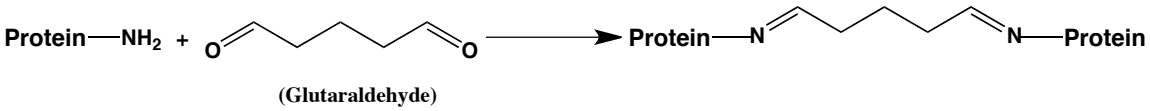

(2)

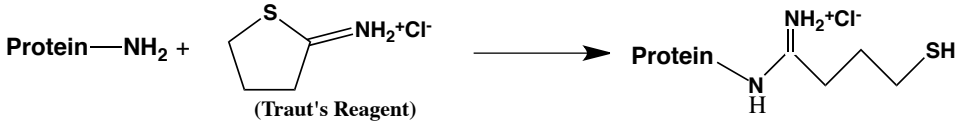

(3)

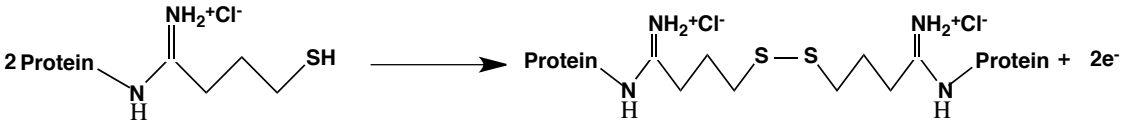

(4)

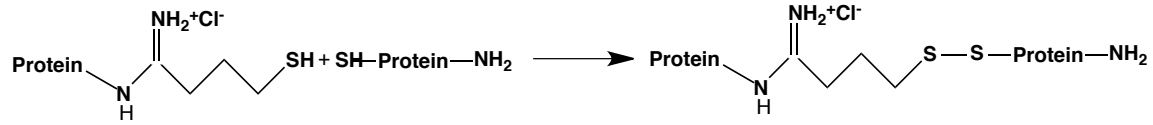

(5)

Chapter 2

General Experimental Methods and Analysis

Materials

Materials were purchased as follows: KCl, 2-iminothiolane•HCl (2IT), terephthalaldehyde (TPDA), and 2-aminoethanethiol from Sigma-Aldrich; sodium L-ascorbate (Asc) and glutaraldehyde from Acros; 2,6-dichlorophenolindphenol (DCPIP) from Encompass chemicals. N_2 was purchased from A-L Compressed Gases. Deinoized water (16.7 MΩ•cm) was purified by a Modu-Pure system and used for rinsing samples and substrates and for preparation of PSI solutions. Gold shot (99.99%) was purchased from J&J Materials. Chromium-coated tungsten filaments were obtained from R.D. Mathis. Silicon (100) wafers (p-doped) were purchased from University Wafers (Boston, MA). An electrochemical sample mask made with plater's tape was purchased from Gamry Instruments. Ethanol was obtained from Decon Labs, Inc. Fresh organic spinach was bought from a nearby grocery store (Harris Teeter).

Profilometry

Profilometry is a technique to measure the thickness of thin films. A Veeco DEKTAK 150 surface profilometer was used to measure the thickness of PSI multilayer films. A cut was made through the PSI multilayer films to the substrate by hand using a lab tweezers so that the bottom line of the valley shows the bare substrate. A high aspect stylus tip scans from one side of the film to the other side across the valley. As the tip follows the contour of the surface, the

vertical displacement of the stylus translates into a sensor's voltage output and shows the thickness profile after appropriate calibration. The measurements were taken over a distance of 800 μm using a stylus with a 12.5 μm radius, applying 1 mg force, and employing a hills-and-valleys detection mode. The reported thickness values and errors represent the averages and standard deviations, respectively, of at least 5 independently prepared films.

Preparation of Gold Substrates and Self-assembled Monolayers (SAMs).

Gold-coated silicon substrates were used as the electrodes in the experiments. To make gold-coated silicon, p-Si (100) wafers were rinsed with ethanol and deionized water, then dried with N_2. Gold-coated silicon substrates were prepared by evaporating chromium (100Å) and Au (1250 Å) in sequence onto the wafers at rates of 1-2 Å/s in a diffusion-pumped chamber with a base pressure of $4*10^{-6}$ torr. After removal from the evaporation chamber, the substrates were cut into 1.2 cm * 3.5 cm pieces. Self-assembled monolayers (SAMs) on gold surfaces were prepared by exposing the gold substrates to 1 mM ethanolic solutions of 2-aminoethanethiol for 1 h. Afterwards, the electrochemical sample masker was used to create a circular area for deposition of PSI films onto a 0.2 cm^2 exposed area of each piece of the SAM-coated substrate.

Photosystem I Extraction and Isolation

PSI from commercial baby spinach was extracted by the method of Reeves and Hall with some adaptations (Figure 5).[12, 31] The thylakoid membrane was removed from the suspension of spinach by centrifugation. PSI complexes were separated from the thylakoid membrane by additional centrifugation. The PSI suspension was purified through column slurry in a chromatographic glass column. PSI effluent was collected into micro centrifuge tubes. To

dialyze PSI and remove surfactants, 1 mL of the column PSI effluent was placed in a 10000 Molecular Weight Cut Off (MWCO) membrane tube that was clipped to seal. The membrane confining the PSI solution was immersed in 2-L deionized water bottle wrapped with aluminum foil to block light. The aqueous solution surrounding the membrane tube was stirred for 24 h to dialyze the PSI solution to remove residual surfactant. The PSI solution in the membrane tube was pipetted into a 2 mL glass vial. After dialysis, the concentration of the extracted PSI solution was approximately 1.6 μM, and the number of externally bound chlorophylls per PSI complex was 71, which was determined by UV-Vis analysis.

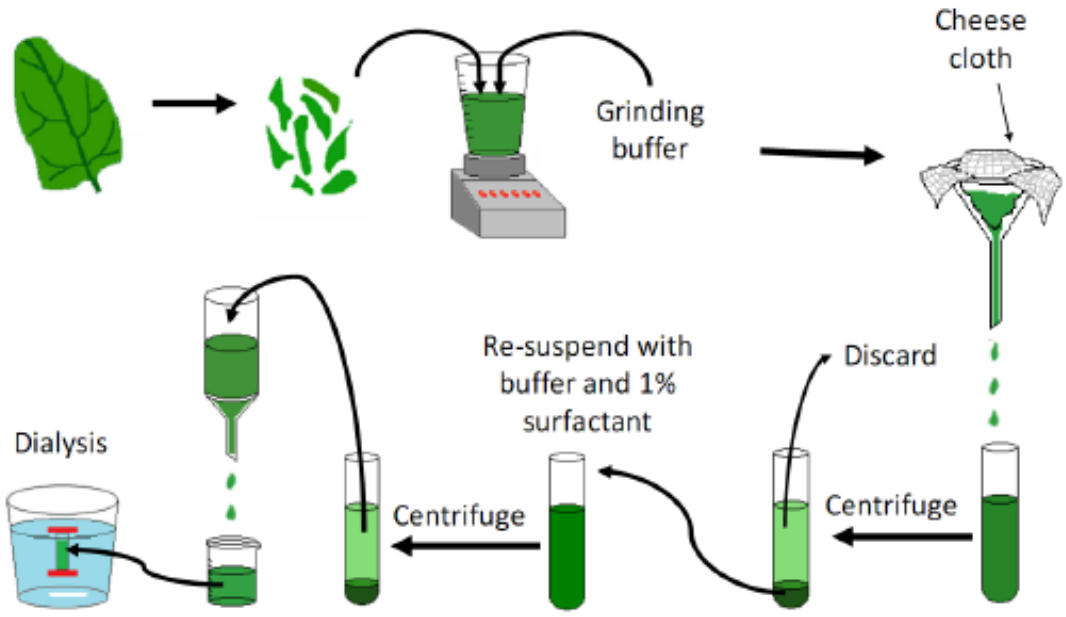

Figure 5. Progress of PSI extraction[2]

Cross-linked PSI Multilayer Assembly

PSI multilayers with/without cross-linkers were prepared by the vacuum-assisted method. 50 μL of PSI solution (1.6 μM) was pipetted onto the exposed area of the SAM-coated gold

substrate containing a mask and placed in the vacuum chamber. The vacuum chamber was sealed and pumped down to a pressure of 30 mTorr for 30 min to evaporate water from the PSI solution. Pure PSI complexes tend to aggregate on the electrode since PSI is the least soluble component in the solution. For the cross-linked PSI films, 50 μL of cross-linker solution (1 mM, aq) was added directly atop the PSI multilayer films after they were dried. Vacuum was again applied to let water evaporate and cross-linker molecules transport throughout the PSI multilayer films. The films were rinsed by DI water afterwards to remove any unreacted cross-linker.

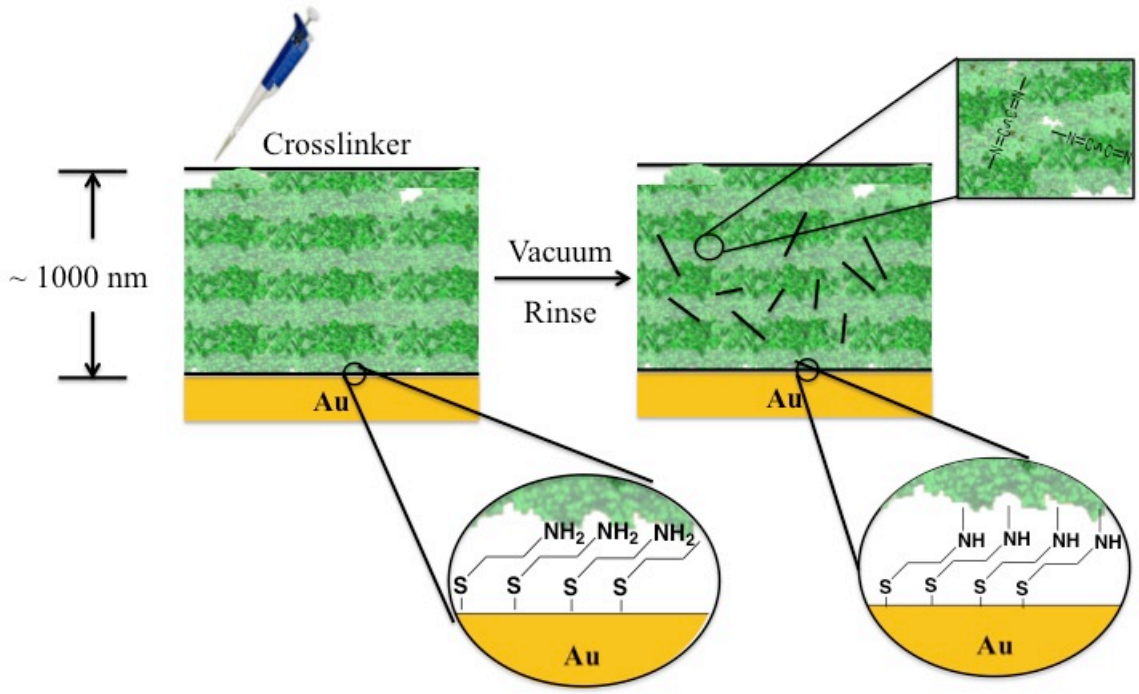

Figure 6. Preparation of cross-linked PSI films on gold substrate

Electrochemical Impedance Spectroscopy (EIS)

Electrochemical Impedance Spectroscopy **(**EIS) is a technique to measure the dielectric properties of a medium over a range of frequencies. EIS involves the application of a small

sinusoidal electrochemical perturbation or voltage. The current of the circuit is directly proportional to the applied voltage and inversely proportional to the resistance of the circuit (Ohm's Law, Eqn. 6).

$$R = \frac{E}{I} \qquad (6)$$

where R is the resistance, E is the electromotive force voltage and I is the current here.

In the EIS, a sinusoidal voltage was applied as Eqn. 7, where the current is shifted in phase ∅ with a phasor notation (Eqn. 8).

$$E(t) = E_0 \, sin\omega t \qquad (7)$$

$$\omega = 2\pi f$$

$$I(t) = I_0 \sin(\omega t + \emptyset) \qquad (8)$$

As a result, impedance could be expressed from Ohm's law shown in the Eqn. 9.

$$Z = \frac{E(t)}{I(t)} = \frac{E_0 sin\omega t}{I_0 \sin(\omega t + \emptyset)} \qquad (9)$$

According to Euler's relationship (Eqn. 10),

$$\exp(j\emptyset) = cos\emptyset + jsin\emptyset \qquad (10)$$

The impedance could be shown as a complex number,

$$Z = \frac{E(t)}{I(t)} = Z_0 \exp(j\emptyset) = Z_0(cos\emptyset + jsin\emptyset) = Z_{Re} + jZ_{Im} \qquad (11)$$

Where $Z_{Re}$is the real part, and $Z_{Im}$is the imaginary part. The Randles equivalent that we have applied is the most common model of electrochemical impedance composing of solution

resistance and a double layer capacitor. The real part impedance is the solution resistance while the imaginary part could be converted from capacitance (Eqn. 12).

$$Z_{Im} = \frac{1}{\omega C_f} \qquad (12)$$

The impedance could be represented in mathematical equation format with the combination of film capacitance (C_f) and resistance (R_f) (Eqn. 13).

$$Z = R_s + \frac{1}{j\omega C_f} \qquad (13)$$

As cross-linker may limit the transfer of ions into the film, by measuring the impedance of the films, we are able to interpret whether the cross-linker functions throughout the film or primarily stays near the film surface. Figure 7 showed the example that how Randle's circuit model was used to fit the frequency-dependent impedance data to determine the solution resistance, as well as film resistance and capacitance. The fitting of the impedance data for PSI films can quantify resistance and capacitance of the films and enable comparison of the different cross-linkers within the PSI films.

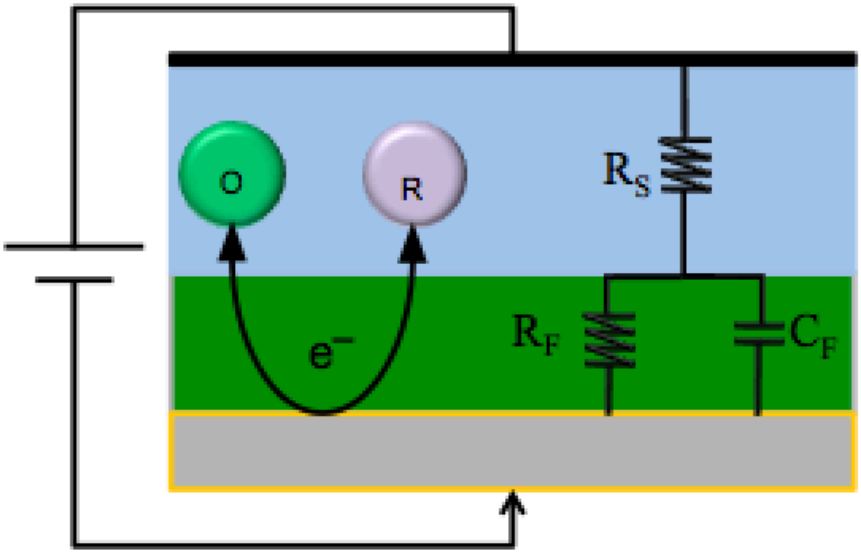

Figure 7. Randle's circuit model

EIS was performed with a Gamry Reference 6000 electrochemical working station. Experiments were performed in a three-electrode electrochemical cell. The system of PSI multilayer film immobilized on the gold substrate was used as the working electrode, and a platinum mesh was used as the counter electrode with an Ag/AgCl reference electrode. An aqueous solution of 1 mM DCPIP/25 mM Asc served as the mediator, and 100 mM KCl was added as supporting electrolyte in the electrochemical cell. An oscillating voltage is applied to the film-coated electrode. All data were collected in the range of 10^{-1} to 10^{4} Hz with 10 points per decade. And current is measured and transformed to impedance by previous equation (Eqn. 8). The data were fit using a Randle's circuit model to determine resistance and capacitance of the films. Reported standard deviations of values were achieved from at least four measurements on independently prepared samples. By comparing the fitting parameters, we can assess the

effective thickness from capacitance and ion transport resistance of the film to quantify the effects of the crosslinking modification.

Photochronoamperometric Measurement

Photocurrent generation scales with the activity and effective integration of PSI protein films. Photochronoamperometry was applied to measure the photocurrent performance of PSI multilayer films immobilized on the gold substrates. Experiments were performed using a CH instruments CHI660a electrochemical workstation. A three-electrode electrochemical cell consisting of a 1 mM DCPIP/ 25 mM Asc(aq) and 100 mM KCl mediator aqueous solution was used. Gold substrates with PSI were used as the working electrode. A platinum mesh was used as the counter electrode and a Ag/AgCl electrode was used as the reference electrode. The photo-response provided in this section was generated by illuminating the sample with a Gebrauch KL 2500LCD lamp at light approximate intensity of ~95 mW/cm^2.

Fourier Transform Infrared Spectroscopy (FT-IR)

Fourier transform infrared spectroscopy (FT-IR) in reflectance mode is a technique to obtain the molecular structure and composition of a film on a surface. An FT-IR spectrometer simultaneously collects spectral data in a wide spectral range. By measuring how well a sample absorbs infrared light at each wavelength, the technique can identify the composition of the materials, and peak shifts are used to correlate with film crystallinity. In this research, the IR beam is achieved from a reflective substrate that is coated by an unmodified PSI film. Molecular groups within the film absorb the IR radiation to yield absorbance peaks in the spectrum with intensities that depend on the concentration of those groups within the films and orientation of

their transition dipole moments. For the PSI film, amide (N-C=O) stretching exists widely in the protein complex. Amide I (1600-1700 cm^{-1}) and Amide II (~1500 cm^{-1}) are the two significant vibrational bands of the stretch. The main peak, the Amide I group, can be deconvoluted into several minor peaks by a Lorentzian curve fitting. These minor peaks correspond to different elements of secondary structure within the protein film. The secondary structure peak assignments were made according to the Table 1 below. By comparing the IR spectrum of different PSI films, we can determine the structure of the proteins and assess whether the protein secondary structure has been altered.[32]

Table 1. Secondary structure peak assignments[33-40]

	β Turn	β Sheet	Unordered Helix	α Helix
Wavelength (cm^{-1})	1616-1620 1680-1690	1624-1636 1692-1697	1638-1645	1648-1660 1663-1667

Chapter 3

Results and Discussion

Thickness and Topography

The PSI multilayer films were prepared onto gold substrates as described in Chapter 2. A 50 μL solution of cross-linker (either 2-IT, TPDA, or GA at 1 mM) was added to the surface of a PSI film to cross-link PSI protein multilayer films before applying vacuum to gradually remove residual water. After PSI films fixed by cross-linker, the films with/without cross-linking were exposed to a vial containing 20 mL of 100 mM KCl (aq) for 12 h. By imitating the environment of the mediator aqueous solution, the exposure could remove PSI complexes and clusters that are not stably immobilized on the surface to investigate the effectiveness of the cross-linker in maintaining PSI film thickness. A profilometer was used to measure the PSI film thickness and, in turn, assess the stability of film thickness to the exposure conditions. In our experiment, the thickness of all the PSI films prepared on amine terminated substrates ($H_2N(CH_2)_2S$/Au) were measured before and after exposure to 100 mM KCl (aq)**.** The thicknesses of all the films range from 1100 – 1350 nm before exposure to aqueous solution, while the thicknesses vary after exposure. Figure 7 compares the percentage of thickness remaining after exposure for an uncross-linked control film with films modified by three different cross-linkers. Cross-linked PSI films lose from ~5 to 20% of film thickness during exposure while the non cross-linked control films lose ~50% of the film thickness, suggesting that cross-linkers help stabilize PSI complexes in these films. In comparing the cross-linkers, considering the error bar of each result,

the percentage of thickness remaining for PSI films fixed by cross-linkers was statistically similar.

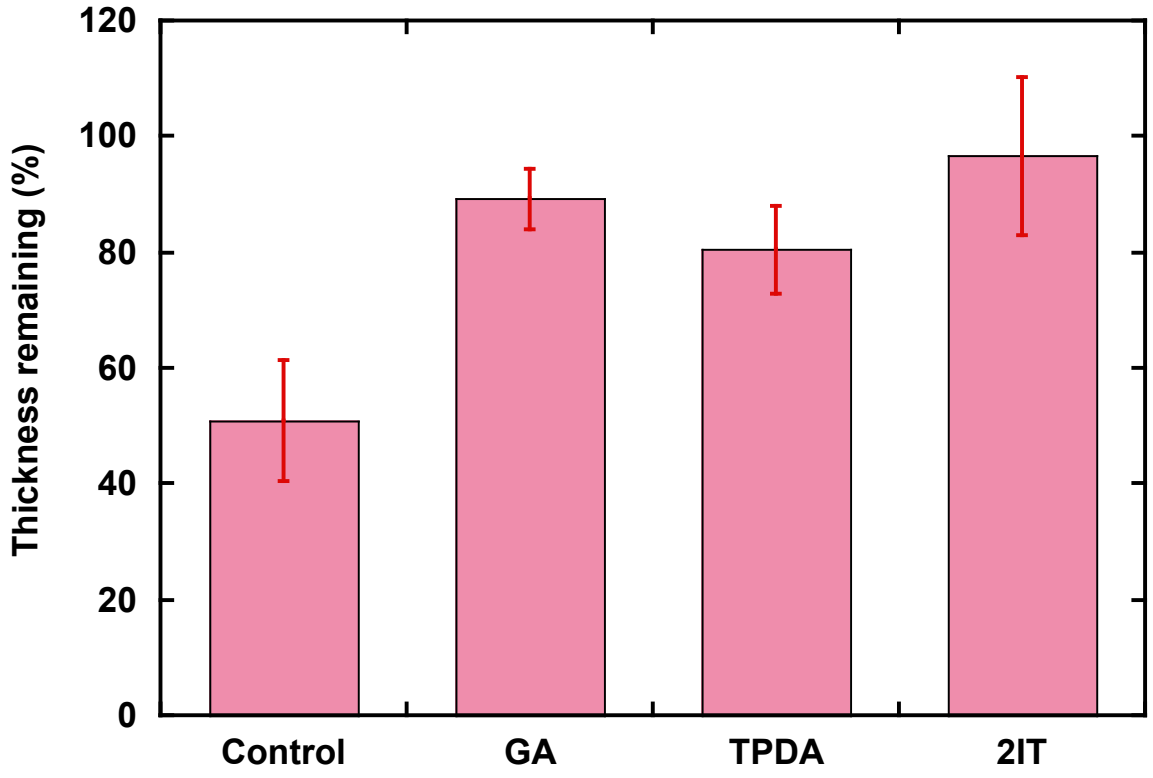

Figure 8. PSI film thickness remaining after exposure to 100 mM KCl (aq) for 12 h.

To employ PSI multilayer films as light-harvesting components in solid-state devices is a promising area of research in the future. Smooth, uniform PSI surfaces could be important to build solid-state devices on PSI films. We examined the effect of cross-linkers on the film surface roughness by obtaining the surface morphology via profilometry (Figure 9). The images of the film surfaces fixed by 2 IT (Figure 9a) and GA (Figure 9b) show roughnesses and uniformity similar to the surface of the uncross-linked control film (Figure 9d). Their profiles show fewer peaks and valleys than the TPDA fixed film. As seen from the line scans, the surface

of the film modified by TPDA is rough with higher peaks than either the control or those modified by 2IT and GA. In addition, the optical images show that there are white crystals on the surface of the TPDA-modified PSI film, with dark clusters dispersed. The rough topography of the TPDA cross-linked films is due to the low solubility of TPDA, yielding insoluble TPDA crystals embedded into the top of the film surface that are difficult to rinse away. Due to the low solubility of TPDA and its effects to promote film roughness, we focused the remaining experiments on GA and 2IT as cross-linkers.

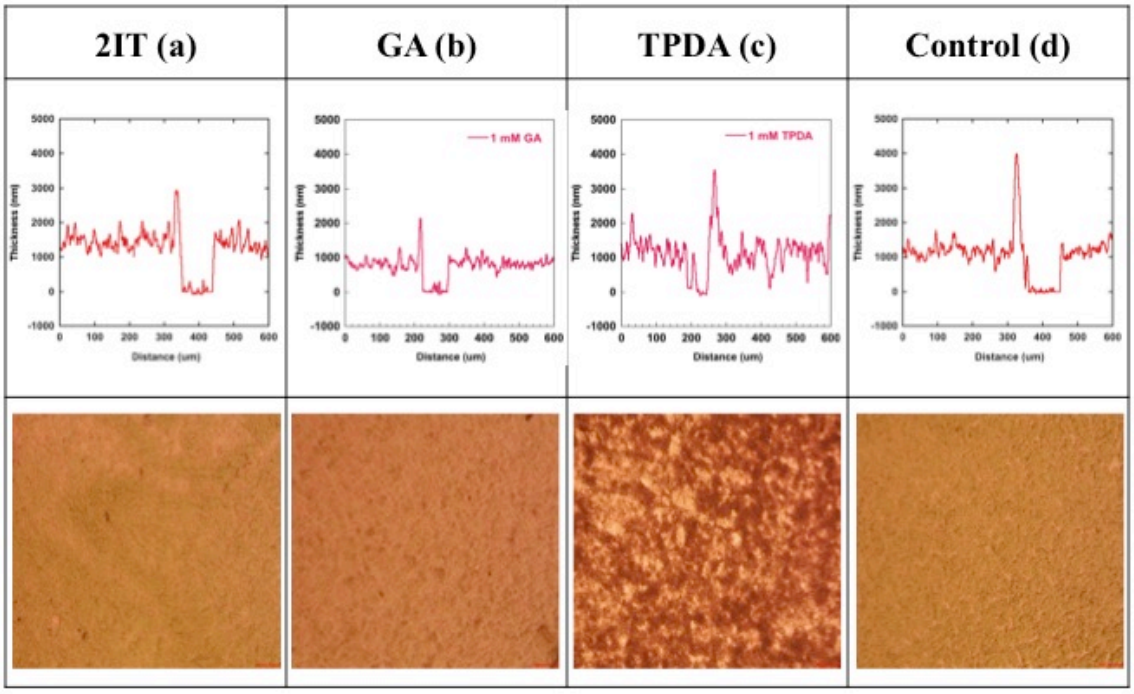

Figure 9. Profilometry scans and optical microscopy images (10 x) of the PSI film surface (bottom row) modified by different cross-linkers, (a) 1 mM 2IT reagent; (b) 1 mM GA; (c) 1 mM TPDA; (d) Control

The Effect of Cross-linker on the PSI Film for a Longer Time Exposure

After verifying the effectiveness of 2IT and GA on the stability of PSI films after 12 h exposure to aqueous solution, we investigated the effect of these cross-linkers on the stability of PSI films over the long time exposure (Figure 10). Both PSI films fixed by 1 mM 2IT and GA were exposed in 100 mM KCl aqueous solution for 72 h, and the thicknesses of cross-linked and control films were examined by profilometry at particular times over this period. From Figure 10, the thickness is similar for PSI films cross-linked by 1 mM 2IT and GA, and both of them show a much higher percentage of protein retained as compared to the uncross-linked control. The thicknesses for all films decreased over the first 10 h, which is consistent with the solubilization of some proteins that were not stabilized, whether via lack of crosslinking or inter protein interactions into the aqueous solution. The thickness remaining for both cross-linked samples (about 80%) was much higher than that of non cross-linked films (about 40%) after exposure to the aqueous solution over the first 20 h. After 20 h, the thicknesses of the films remained constant. That 60% of the control film is lost suggests that some monomeric PSI proteins are poorly stabilized by physical interactions and tend to desorb from the film into the 100 mM KCl (aq) solution. Cross-linking by GA and 2IT stabilizes approximately two thirds of these mobile proteins and prevents further proteins from desorbing for up to three days of exposure.

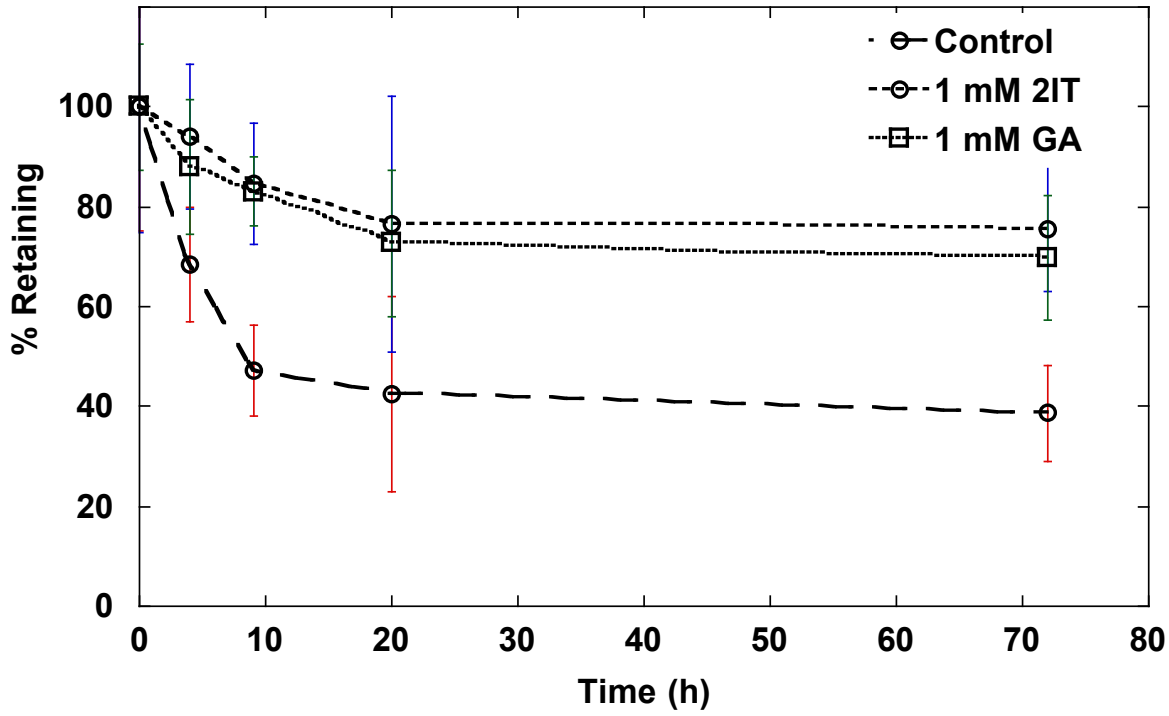

Figure 10. The percentage of PSI films retained after exposure to 100 mM KCl (aq) for three days.

The dissolution rate of the films has been investigated. The dissolution of multilayer PSI protein films to aqueous solution could be simplified as a first order reaction model. Assume the dissolution rate is constant for each film, rate constant could be achieved by regression fitting with first order reaction equation (Eqn. 14), where the coverage θ was regarded as film mass. Since the thickness remained consistent after 20 h, only first four points had been considered in the fitting.

$$\frac{d\theta}{dt} = -k_t\theta \qquad (14)$$

Table 2 shows the dissolution rate of each PSI film and Figure 11 shows the first-order fitting of thickness lost. The first-order plot indicates that the rate constant of PSI films fixed by 2IT and GA were similar, but the rate constant of the control film was 6-7 times higher than both the cross-linked films. Again this result shows that the dissolution or desorption of PSI proteins from control film was much faster than the cross-linked ones.

Table 2. Dissolution rate of PSI film

	Control	2IT	GA
Dissolution rate (kt)	0.0853	0.0142	0.0172

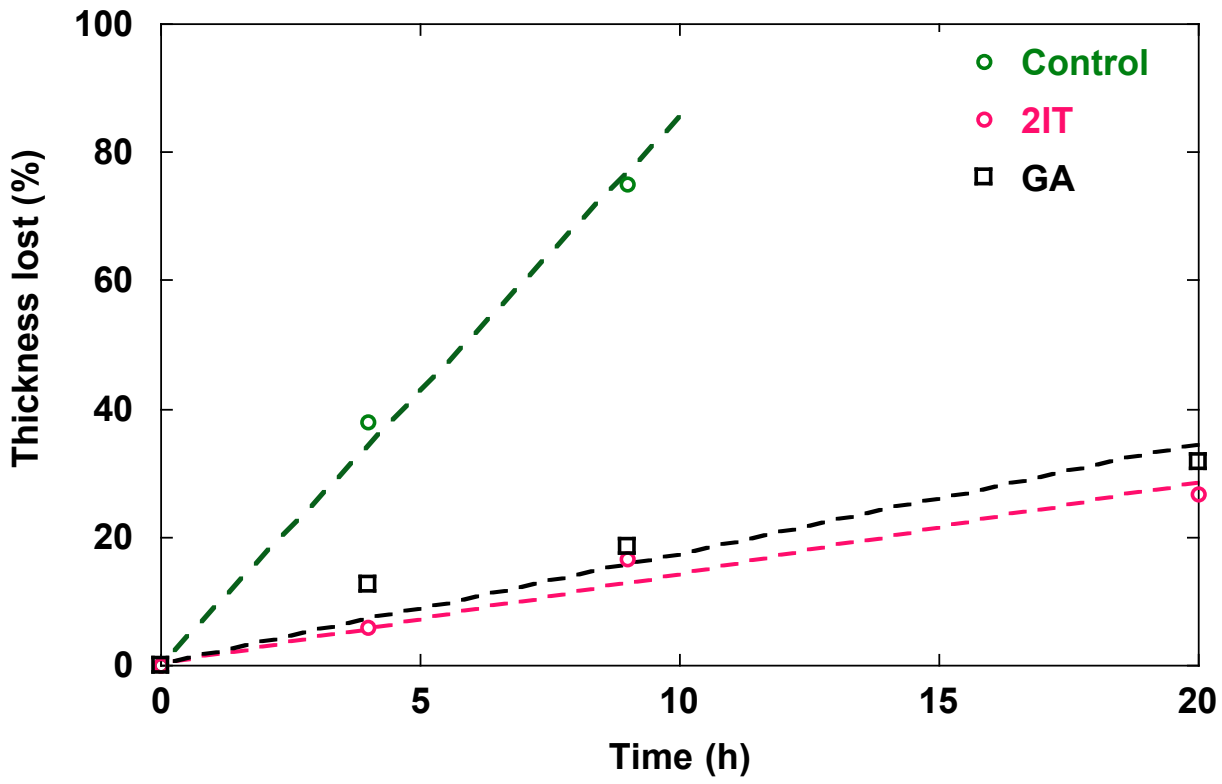

Figure 11. The fitting of thickness lost over 72 h

Electrochemical Impedance Spectroscopy (EIS)

EIS can sensitively characterize ion transfer into thin film, we have applied EIS to characterize PSI films with/without cross-linkers to determine if the presence of cross-linkers alters the barrier properties, such as film capacitance and resistance. After collecting impedance data, a Randle's circuit model[41] was used to fit the data, providing curve fits that are also shown in Figure 5. From the fitting data shown in Table 3, the impedance obtained is similar for the two cross-linked films and is higher than the non cross-linked films, most appreciably at lower frequencies in which sufficient time is provided for ions to diffuse into the film. The resistance R_f of the cross-linked films is 3-5 times greater than the reference films, and their capacitance is only about half of that of the reference films. As the thicknesses of the cross-linked and control films are similar, the reduced C_f of the cross-linked films suggests that the cross-linked films are dryer than the reference films, resulting in a lower effective dielectric constant. The higher resistance and lower capacitance of cross-linked films demonstrate that the cross-linking provides modest barriers within the films to limit the transport of water and ions. The behavior of all the impedance spectra to match a single-time-constant model suggests that the cross-linkers functionalize the films uniformly, and do not form a dense heterogeneous network at the protein/solution interface to limit ion transfer. Such a heterogeneous outer thin film would be expected to yield more complex impedance behavior. The impedance results show that the cross-linkers effectively alter ion transfer throughout the protein film.

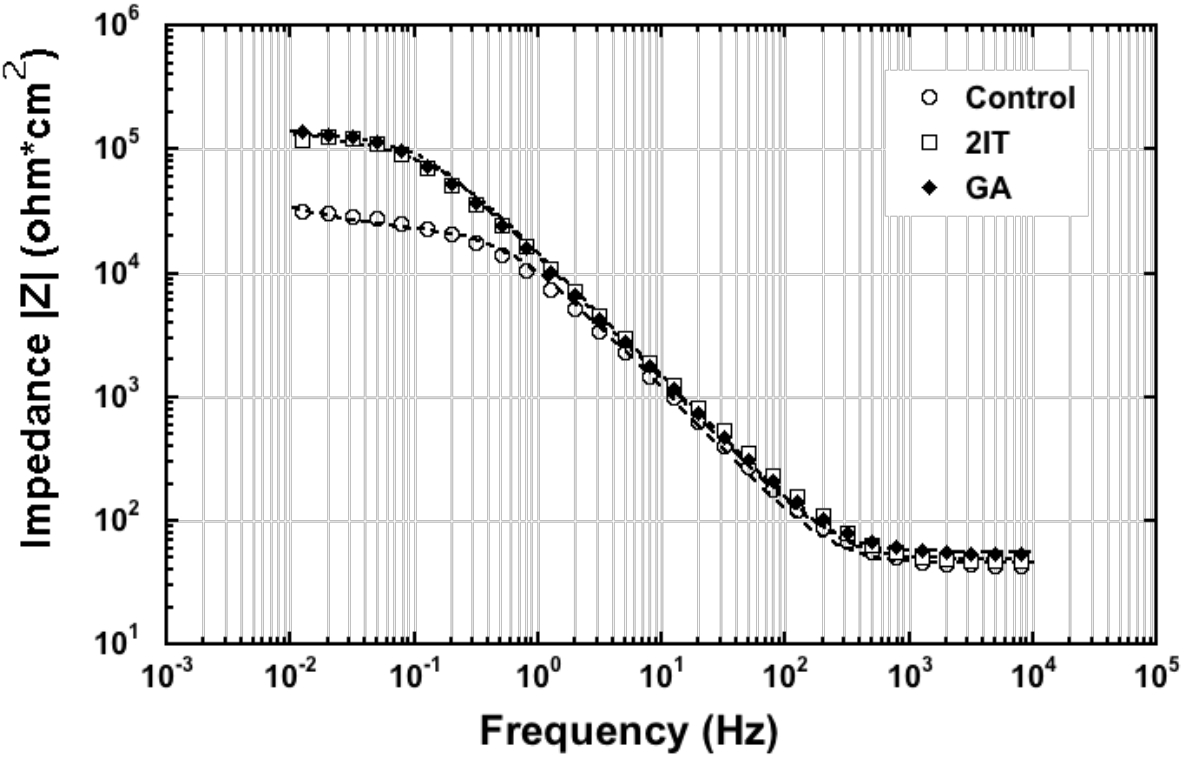

Figure 12. Bode magnitude impedance plot for PSI films that are not cross-linked (control) and those cross-linked by 2IT and GA.

Table 3. Impedance electrical properties of PSI films with/without cross-linker

	Rs (ohm*cm^2)	Cf (10^6 F/cm^2)	Rf (10^3 ohm/cm^2)
Control	42	21	30
2IT	49	11	98
GA	56	12	132

Infrared Spectroscopy of PSI Multilayer Films

PSI multilayer films fixed by 1 mM 2IT and GA were characterized by reflectance infrared spectroscopy (Figure 13). It showed that a small peak existed at 1400 cm^{-1} for the 2IT-fixed film. The films were rinsed by DI water and IR test was performed again. The peak disappeared from the 2IT fixed films then. This could be the excess 2IT within the PSI film that

was rinsed away. And both PSI films fixed by GA and 2IT exhibited similar IR spectra compared with that of control film. All the scans showed identical peaks in the Amide I (1700-1600 cm^{-1}) and Amide II (~1500 cm^{-1}) regions as compared with the control film. 1 mM cross-linker does not change the main structure of PSI proteins from the spectra.

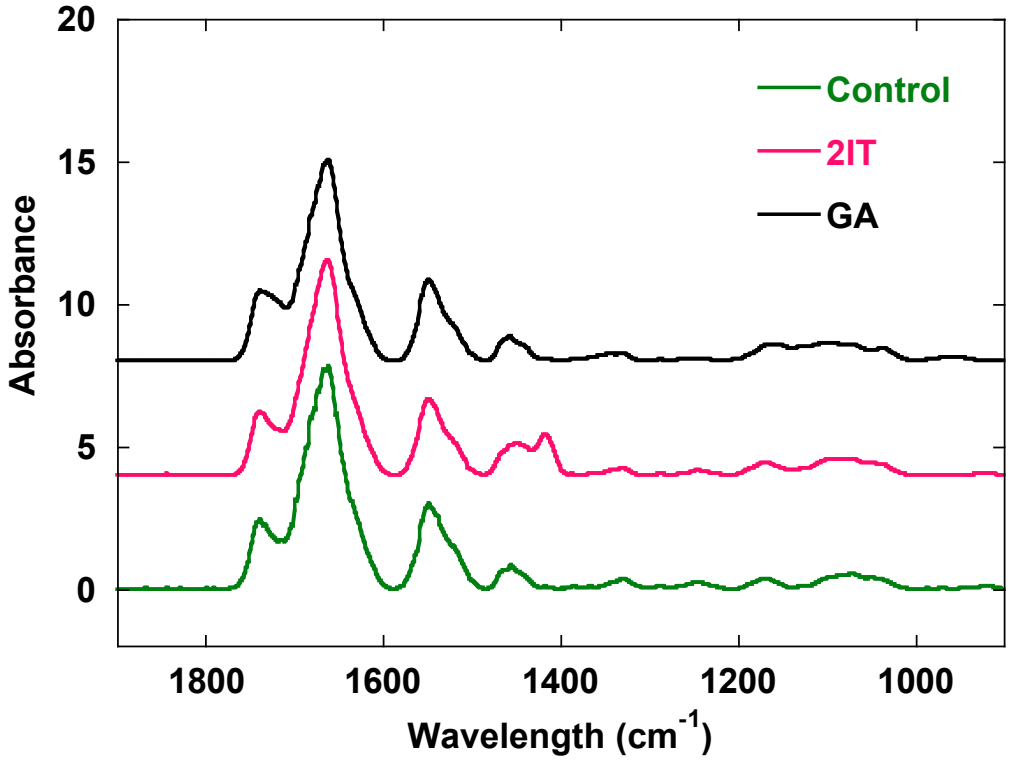

Figure 13. IR Spectra of PSI films fixed by 2IT, GA and control

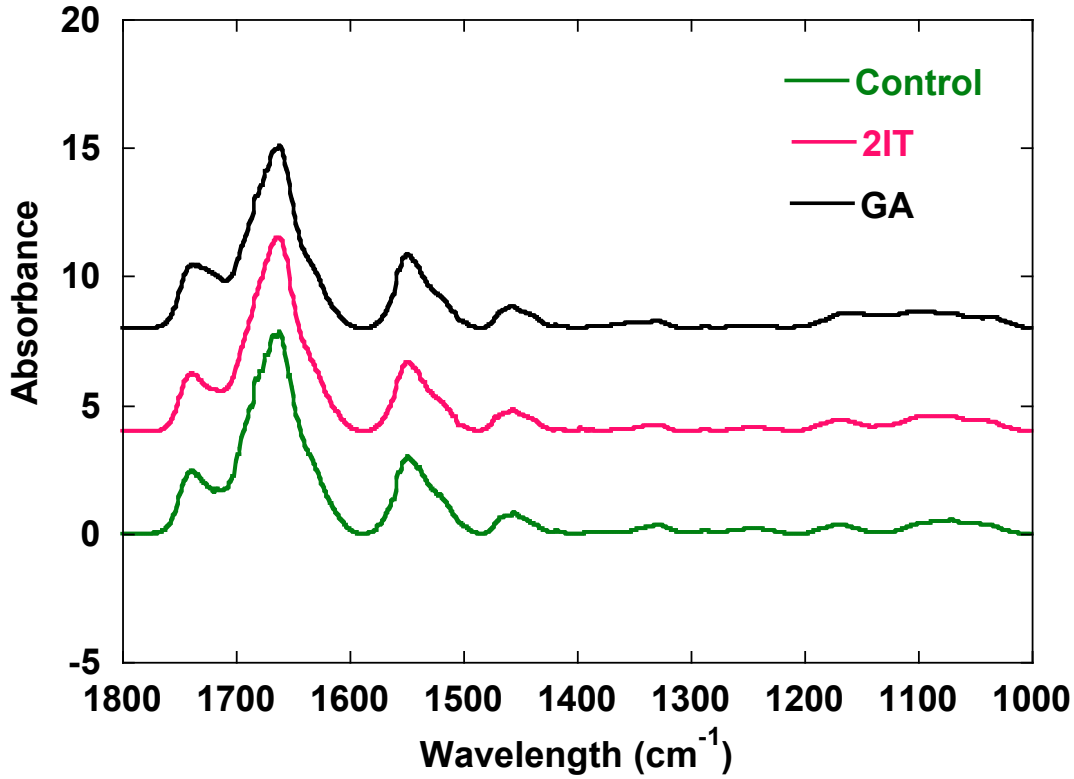

Figure 14. IR spectra of PSI films fixed by 2IT, GA and control after rinsing by DI water

Secondary structure of PSI was determined by deconvolution the Amide I absorption peak by MATLAB. Table 4 displays the percentage of each secondary structure in Amide I from different sample. The result showed that the percentage of β-sheet and unordered helix was similar and the percentage of β-turn and α-helix had small difference. The cross-linker may change the structure of the PSI protein to a small extent.

Table 4. Percentage of secondary structure assignment, estimated to be accurate within ±5%

	Control	2IT	GA
β-turn	19	23	18
β-sheet	38.	39	39
unordered helix	13	14	12
α-helix	30	24	31

Electrochemical Photochronoamperomety Measurement

Photocurrent performance scales with the amount of PSI in the film[22], its activity, and its accessibility by diffusible mediators . To investigate the photoelectrochemical activity of PSI films after cross-linking, photochronoamperomety measurements were performed at an open circuit potential (no over potential) to ensure the same driving force is provided for all systems. When the films are irradiated by light, photocurrent is generated, as the PSI complexes are able to pull electrons from the electrode and deliver them to redox mediators in solution. We used dichlorophenolindophenol (DCPIP) as the electron acceptor and sodium ascorbate as a sacrificial electron donor, with an illumination time of 20 s. In response to the irradiation, cathodic current is generated from the PSI films. The data shown in Table 5 are the photocurrents obtained 10 s after illumination. As shown in Figure 15 and in Table 5, the photocurrents generated by the non cross-linked control film and the film fixed by 2IT have similar magnitude, which is around 4 $\mu A/cm^2$, while the one fixed by GA exhibits greatly reduced photocurrent. We expect that the strong reactivity of GA with proteins may lead to some damaging modifications[24] that inhibit electron transfer to or through the protein and/or from PSI to mediator species.

Table 5. Photocurrent of PSI multilayer films with/without cross-linker

	Photocurrent ($\mu A/cm^2$)	i_{CL}/i_{ref} (100%)
Control	4.03 ± 0.61	100 ± 15
2IT	4.10 ± 0.69	102 ± 17
GA	1.22 ± 0.28	30 ± 23

In addition, we have compared the photocurrent generation of PSI films with/without cross-linker before and after exposure to 100 mM KCl (aq) for 3 days to assess the stability of photocurrent for these films (Figure 16). The photocurrent generated by the PSI films fixed by 2IT is similar at ~4 $\mu A/cm^2$ both before and after exposure, while that generated by the control films decreased by 2 - 3 fold. The greater amount of PSI lost from the non crossed-linked films (Figure 10) is consistent with the stronger decrease of the photocurrent, as we have previously shown that PSI film thickness and photocurrent are positively correlated.[22] For the PSI films fixed by GA, photocurrent remained nearly constant after three days, although the magnitude was lower than that fixed by 2IT due to the presumed damage of the protein by GA. The 20% loss of thickness in 2IT stabilized PSI films (Figure 10) does not result in measurable loss in photocurrent (Figure 16). This observation suggests that the small fraction lost from the 2IT-fixed film was not integral to photocurrent production by the film.

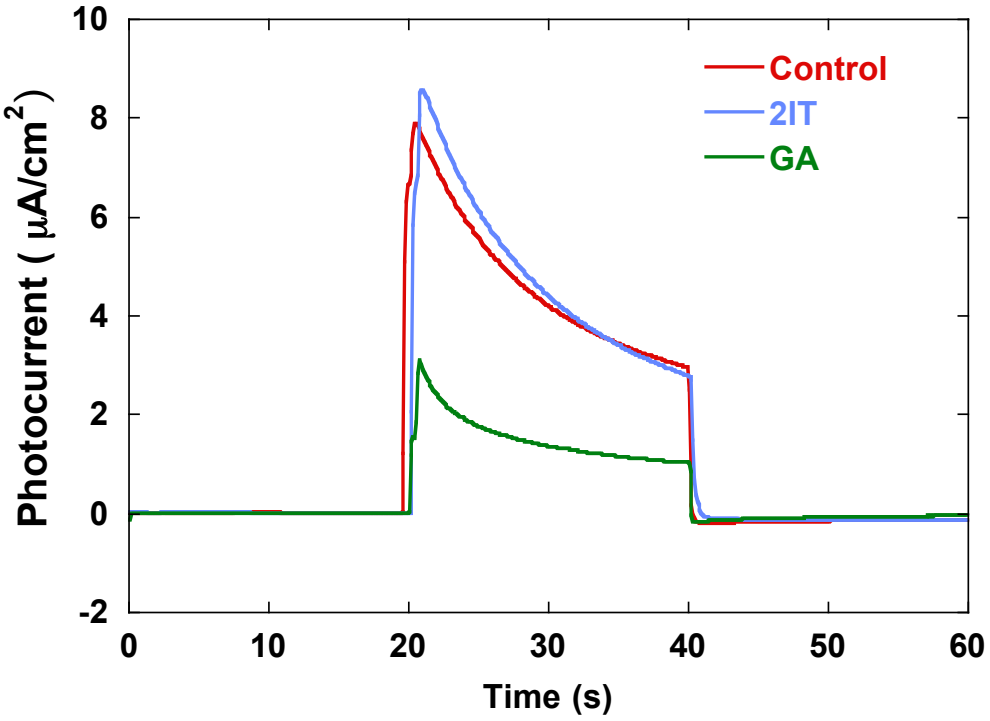

Figure 15. Photocurrent of PSI films before KCl (aq) exposure

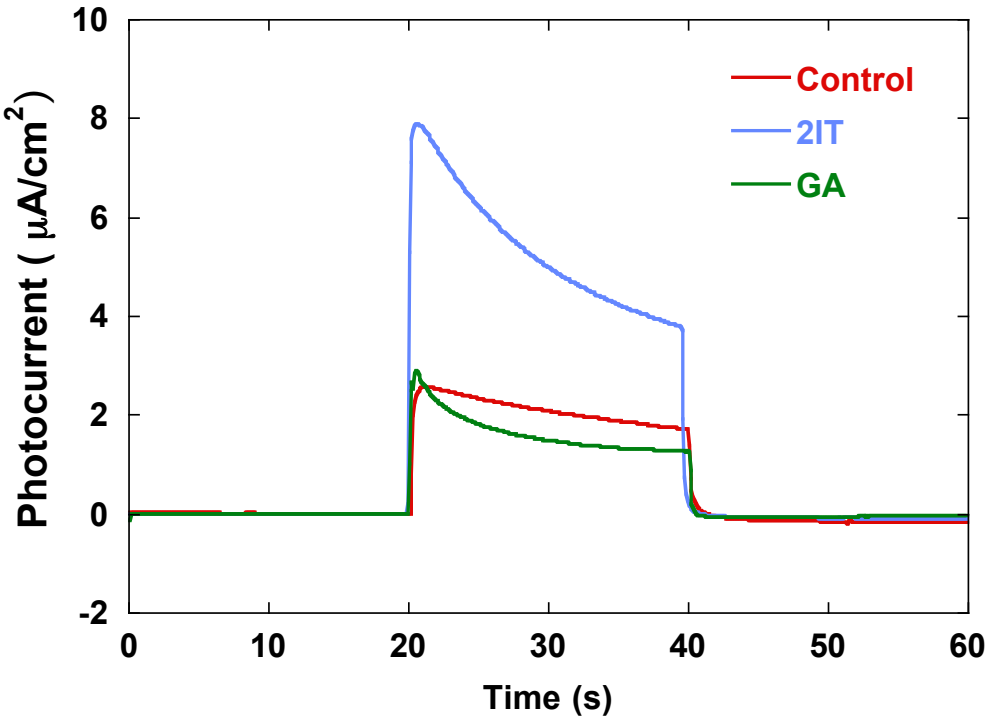

Figure 16. Photocurrent of PSI films after KCl (aq) exposure for 3 days

Conclusion

Cross-linkers that covalently link the abundant lysine residues within a PSI multilayer film have been investigated. The stability of cross-linked films can be increased both in the thickness and photocurrent, but the overall performance depends on the properties of the cross-linkers. Cross-linkers with very low solubility similar to TPDA can crash out onto the surface of the film and hamper uniformity, and cross-linkers like glutaraldehyde that have strong reactivity can reduce the activity of the proteins. Out of the three cross-linkers investigated, 2-iminothiolane (2IT) has optimal properties to improve the stability of the PSI film while maintaining the photocurrent of the film. Small (1mM) amounts of 2IT can maintain the photocurrent generation over at least 3 days as well.

Reference

1. W. J. S. D. Joseph A. Berry, *Environmental Regulation of Photosynthesis*. (Academic Press, INC, New York, 1982).
2. D. R. Hall, K. , *Photosynthesis*, 6th ed ed. (Cambridge University Press, Cambridge, U.K., 1999).
3. J. Golbeck, *Photosystem I: the light-driven plastocyanin: ferredoxin oxidoreductase.* (2006).
4. L. Frolov, O. Wilner, C. Carmeli and I. Carmeli, Advanced Materials **20** (2), 263-266 (2008).
5. M. Ciobanu, H. A. Kincaid, V. Lo, A. D. Dukes, G. Kane Jennings and D. E. Cliffel, Journal of Electroanalytical Chemistry **599** (1), 72-78 (2007).
6. A. K. Badura, T.; Schuhmann, W.; Rogner, M. Energy Environ. Sci. 2011, 4, 3263–3274.
7. E. Greenbaum, Science **230,**, 1373–1375 (1985).
8. E. Greenbaum, Appl. Biochem. Biotechnol. **20-21**, 813–824 (1989).
9. D. Mukherjee, M. May, M. Vaughn, B. D. Bruce and B. Khomami, Langmuir **26** (20), 16048-16054 (2010).
10. A. Lovins, *Winning the oil endgame: innovation for profits, jobs and security*. (Rocky Mountian Institute, 2004).
11. e. Amunts, (Photosynthesis Research, 2007), Vol. 91(2-3), pp. 151.
12. M. Ciobanu, H. A. Kincaid, G. K. Jennings and D. E. Cliffel, Langmuir **21** (2), 692-698 (2004).
13. G. L. Darlene Gunther, David E. Cliffel, and G. Kane Jennings, Industrtrial Biotechnology **9** (1), 37-41 (2013).
14. D. Gunther, G. LeBlanc, D. Prasai, J. R. Zhang, D. E. Cliffel, K. I. Bolotin and G. K. Jennings, Langmuir **29** (13), 4177-4180 (2013).
15. H. A. Kincaid, T. Niedringhaus, M. Ciobanu, D. E. Cliffel and G. K. Jennings, Langmuir **22** (19), 8114-8120 (2006).
16. P. N. Ciesielski, F. M. Hijazi, A. M. Scott, C. J. Faulkner, L. Beard, K. Emmett, S. J. Rosenthal, D. Cliffel and G. Kane Jennings, Bioresource Technology **101** (9), 3047-3053 (2010).
17. A. K. Manocchi, D. R. Baker, S. S. Pendley, K. Nguyen, M. M. Hurley, B. D. Bruce, J. J. Sumner and C. A. Lundgren, Langmuir **29** (7), 2412-2419 (2013).
18. P. Kiley, X. Zhao, M. Vaughn, M. A. Baldo, B. D. Bruce and S. Zhang, PLoS Biol **3** (7), e230 (2005).
19. A. Mershin, Matsumoto, Kazuya, Kaiser, Liselotte, Yu, Daoyong, Vaughn, Michael, Nazeeruddin, Md. K., Bruce, Barry D., Graetzel, Michael, Zhang, Shuguang, in *Scientific Reports* (2012), Vol. 2.
20. C. J. Faulkner, S. Lees, P. N. Ciesielski, D. E. Cliffel and G. K. Jennings, Langmuir **24** (16), 8409-8412 (2008).
21. P. N. Ciesielski, A. M. Scott, C. J. Faulkner, B. J. Berron, D. E. Cliffel and G. K. Jennings, ACS Nano **2** (12), 2465-2472 (2008).

22. P. N. Ciesielski, C. J. Faulkner, M. T. Irwin, J. M. Gregory, N. H. Tolk, D. E. Cliffel and G. K. Jennings, Advanced Functional Materials **20** (23), 4048-4054 (2010).
23. G. LeBlanc, G. Chen, E. A. Gizzie, G. K. Jennings and D. E. Cliffel, Advanced Materials **24** (44), 5959-5962 (2012).
24. A. F. S. A. Habeeb and R. Hiramoto, Archives of Biochemistry and Biophysics **126** (1), 16-26 (1968).
25. G. LeBlanc, K. M. Winter, W. B. Crosby, G. K. Jennings and D. E. Cliffel, Advanced Energy Materials **4** (9), n/a-n/a (2014).
26. A. H. Korn, S. H. Feairheller and E. M. Filachoine, Journal of Molecular Biology **65** (3), 525-529 (1972).
27. A. C. N. a. H. N. R. Paul M. Hardy, J. Chem. Soc., Perkin Trans. 1, 958-962 (1976).
28. G. Bulaj, Biotechnology Advances **23** (1), 87-92 (2005).
29. M. J. McCall, H. Diril and C. F. Meares, Bioconjugate Chemistry **1** (3), 222-226 (1990).
30. R. Jue, J. M. Lambert, L. R. Pierce and R. R. Traut, Biochemistry **17** (25), 5399-5406 (1978).
31. D. O. H. S.G. Reeves, Methods Enzymol **69** (85) (1980).
32. S. M. Gilbert, N. Wellner, P. S. Belton, J. A. Greenfield, G. Siligardi, P. R. Shewry and A. S. Tatham, Biochimica et Biophysica Acta (BBA) - Protein Structure and Molecular Enzymology **1479** (1–2), 135-146 (2000).
33. T. Heimburg, J. Schünemann, K. Weber and N. Geisler, Biochemistry **38** (39), 12727-12734 (1999).
34. R. A. Moore, S. F. Hayes, E. R. Fischer and S. A. Priola, Biochemistry **46** (24), 7079-7087 (2007).
35. J. F. Kang, A. Ulman, S. Liao and R. Jordan, Langmuir **15** (6), 2095-2098 (1999).
36. X. Ruan, J. Wei, Q. Xu, J.-s. Wang, Y.-d. Gong, X.-f. Zhang, T.-y. Kuang and N.-m. Zhao, Journal of Molecular Structure **525** (1–3), 97-106 (2000).
37. J. T. Pelton and L. R. McLean, Analytical Biochemistry **277** (2), 167-176 (2000).
38. K. Fu, K. Griebenow, L. Hsieh, A. M. Klibanov and L. Robert, Journal of Controlled Release **58** (3), 357-366 (1999).
39. N. P. Camacho, S. Rinnerthaler, E. P. Paschalis, R. Mendelsohn, A. L. Boskey and P. Fratzl, Bone **25** (3), 287-293 (1999).
40. J. L. R. Arrondo and F. M. Goñi, Progress in Biophysics and Molecular Biology **72** (4), 367-405 (1999).
41. S. Pan and L. Rothberg, Langmuir **21** (3), 1022-1027 (2005).

Appendix

Aside from the stability of PSI films exposed to aqueous solutions, as in a wet cell, I have investigated the stability of PSI films exposed in air at different temperatures and in organic solvents. I will discuss some preliminary results about the stability of these films in these two parts. In addition, I have performed some analysis of PSI multilayer films on p-Si substrates.

The Stability of PSI Multilayer Films to Different Solvents

The stability of PSI proteins to different solvents has also been investigated. First, solid PSI proteins were extracted by centrifugation; then the extracted solid was dissolved in small tube with different organic solvents, including ethyl acetate (EA), tetrahydrofuran (THF) and dichloromethane (DCM). Same volume of organic solvent was added to each tube to make sure the PSI concentration was similar to the original aqueous suspension. PSI films were made by drop casting the solution on a gold substrate over night. This re-suspending process was shown in Figure A-1. Film thicknesses were detected by profilometry (Figure A-2).

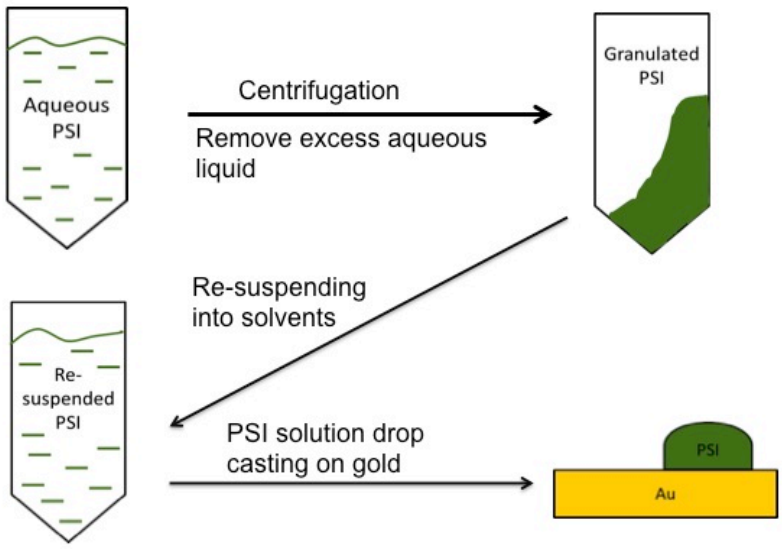

Figure A- 1. Re-suspending Procedure

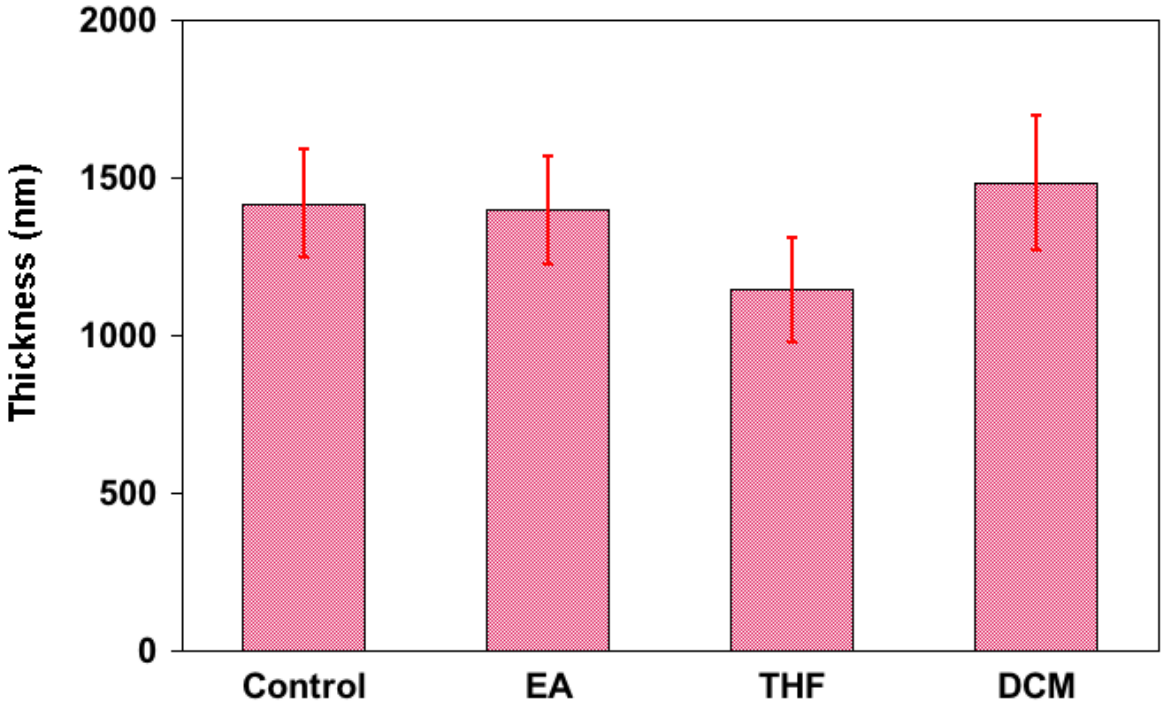

Figure A- 2. Thickness of PSI films that were dissolved into organic solvents and then drop casted onto gold substrates

Due to the similar PSI concentration compared to the original aqueous solution, the thickness of PSI proteins dissolved in the organic solvents is similar to the aqueous control. Photocurrent performance of the films dissolved into different solvents has been investigated (Table A-1). It elucidated that PSI films dissolved in organic solvents generated photocurrent in similar magnitude, which means the organic solvent did not damage the activity of the protein.

Table A- 1. Photocurrent of PSI multilayer films dissolved into organic solvents. These data are based on one measurement of one sample

	Photocurrent ($\mu A/cm^2$)
Control	4.0
DCM	5.1
EA	4.2
THF	3.5

Also, I have used FT-IR to check the IR spectra of the PSI films made by the re-suspending method. Figure A-3 shows the spectra of all films have similar Amide I and II regions and similar peak shapes, although the peaks are different in height. The spectra again showed that the films made by re-suspending PSI proteins does not significantly change the secondary structure of the PSI protein within the film. However, both IR scans and photocurrent measurements were just one-time tests; more tests need to be done to confirm the results.

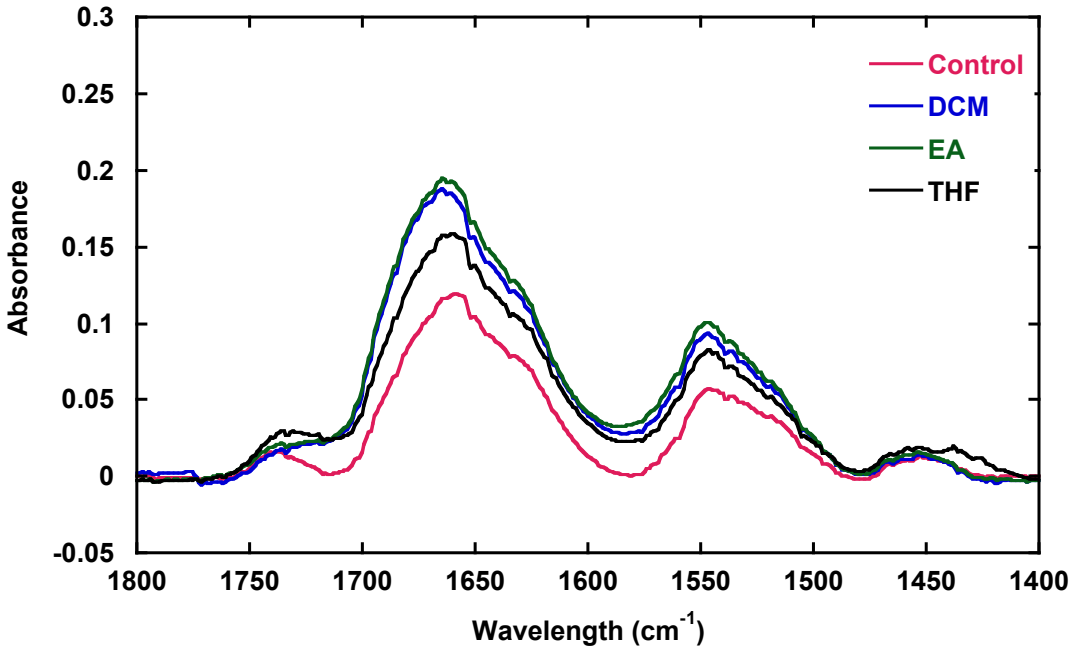

Figure A- 3. FTIR spectra of PSI films dissolved in organic solvents

In addition, PSI proteins dissolved into other organic solvents has been employed to make multilayer films by spin-coating method at varied speeds on gold substrates. However, since the proteins do not have much adhesion with the substrates, the films were thin and relatively rough. The films made by the spin-coating method were exposed in 100 mM KCl (aq) overnight, and their thicknesses were tested before and after exposure to assess their stability. Here we showed the thickness remaining (Table A-2), which indicates that with the higher speed of spin coating, the much easier for the proteins to become lost into aqueous solution.

Table A- 2. Thickness comparison after/before ratio

Speed (RPM)	5% Dodecanol	5% Propanol
~1000	80%	80%
~3000	0	20%

Study of PSI Multilayer Films on p-Si Substrates

The investigation of PSI multilayer films on p-Si was performed in 2013. Using the similar vacuum-assisted method, PSI multilayer films were deposited onto p-Si. EIS was performed to compare the impedance for both bare p-Si (Figure A-3) and PSI-coated p-Si (Figure A-4) in both dark and light conditions. For bare p-Si, the test was performed in light, followed by the dark condition. And same procedure was conducted for another time.

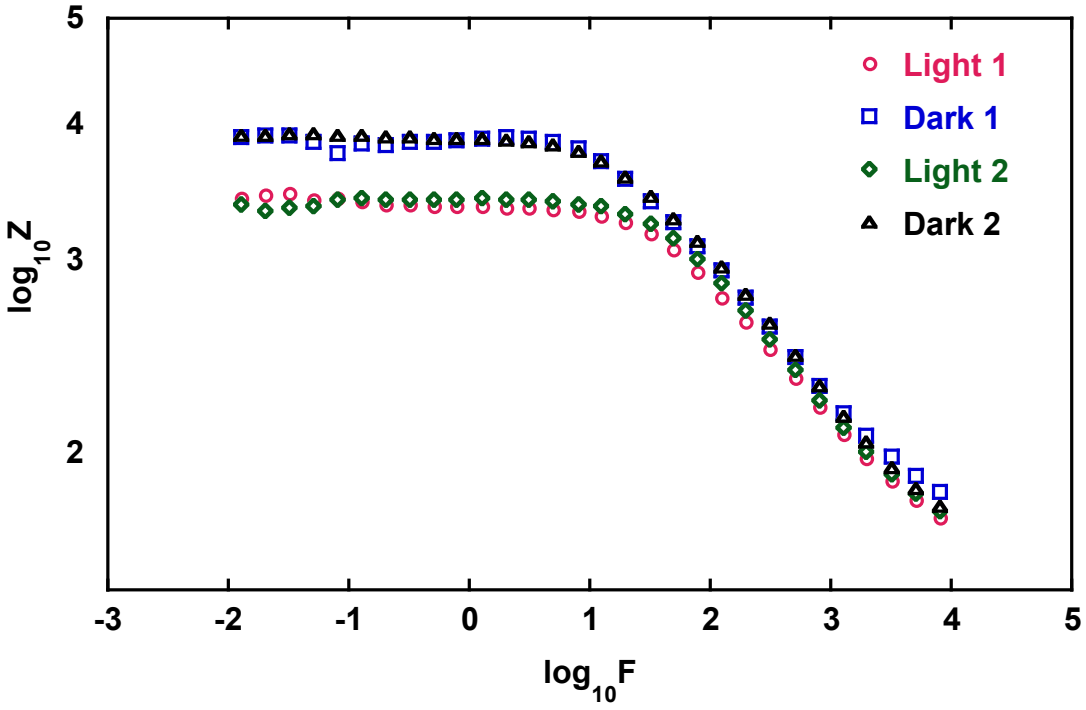

Figure A- 4. Impedance of bare p-Si

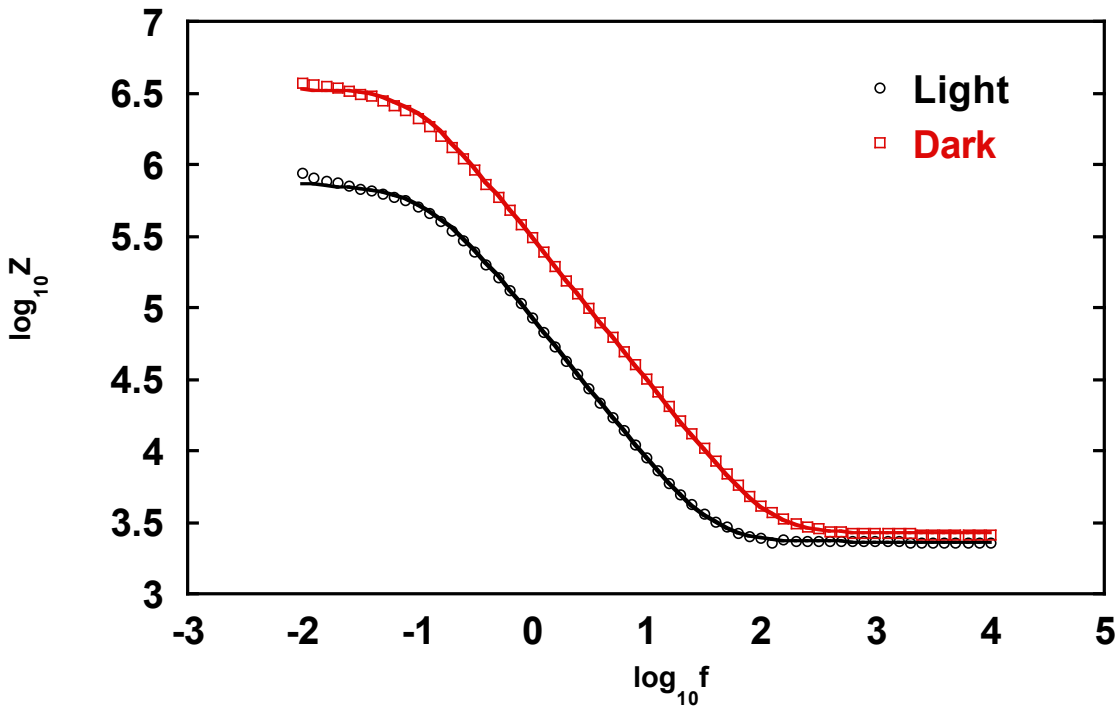

Figure A- 5. Impedance of PSI films on p-Si in light/dark conditions

Due to its photoelectric effect, bare Si generated lower resistance when illuminated. The PSI-modified electrode generated lower resistance when in the light too. In the illuminated condition, PSI draws electrons from p-Si and effectively transfers them to redox species in solution. The resistance of the PSI-modified electrode is higher than that of bare Si, due to the impedance provided by the PSI film.

Functionalization of p-Si with Alkyne-Based Monolayers

A prominent problem with silicon as an electrode for wet cells is that it rapidly oxidizes to greatly reduce photoelectrochemical performance. In an effort to inhibit silicon oxidation for PSI/silicon systems, we have assembled organic monolayer films onto the etched p-Si, including

propiolic acid, mono-propargylamine, and 4-pentyn-1-ol. The molecules have different terminal functional groups to enable different interactions with PSI films (Table A-3).

Table A- 3. Structure and charge of organic molecules

$CH \equiv C - \overset{\overset{O}{\|}}{C} - OH$	Propiolic acid	Negative
$CH \equiv C - CH_2 - NH_2$	Mono-propargylamine	Positive
$CH \equiv C - (CH_2)_3\,OH$	4-Pentyn-1-ol	Neutral

Monolayer films were assembled onto etched Si by exposing etched Si to the particular organic molecule in hexane at 25°C in glass vial, dry N_2 was blown into the vial through the tube to create a positive pressure that blocks the transfer of O_2. The organic monolayer was assembled onto p-Si overnight. PSI multilayer films were deposited onto the organic monolayer surface by the vacuum-assisted method on the second test day. (Figure A-6).

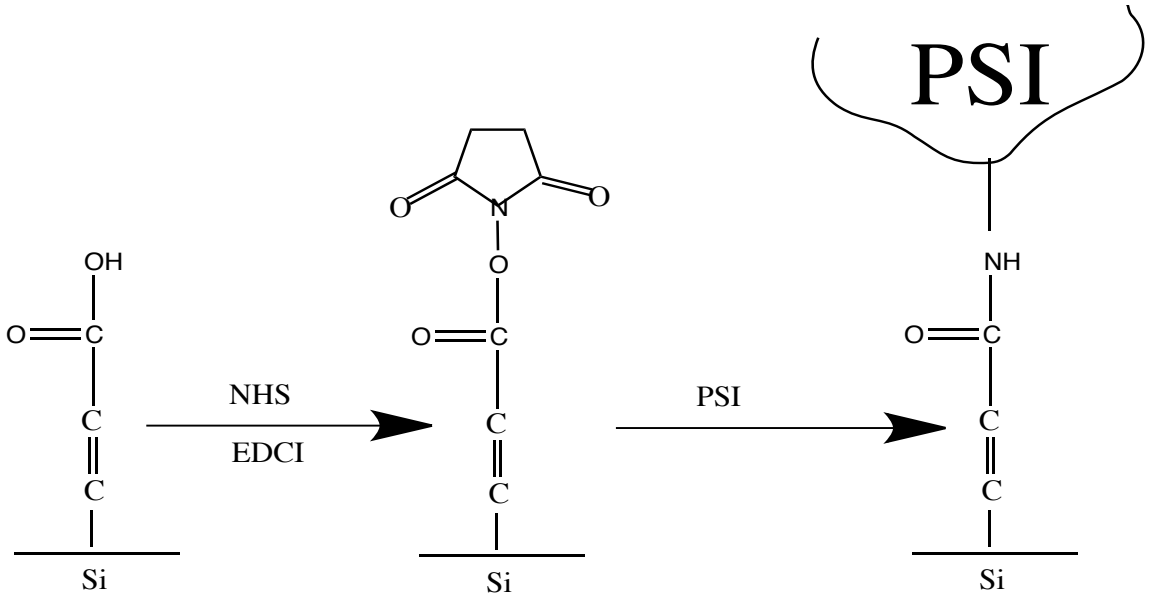

Figure A- 6. The process to fabricate PSI multilayer films on the SAM-Si

Photochronoamperometry was used to measure the photocurrent through the PSI film immobilized on the different organic groups on p-Si under red light. The highest current density, at 50 $\mu A/cm^2$, was achieved using the carboxylic acid monolayer. This result is likely due to electrostatic attraction between the negative surface of the acid monolayer and the positive ends on PSI.

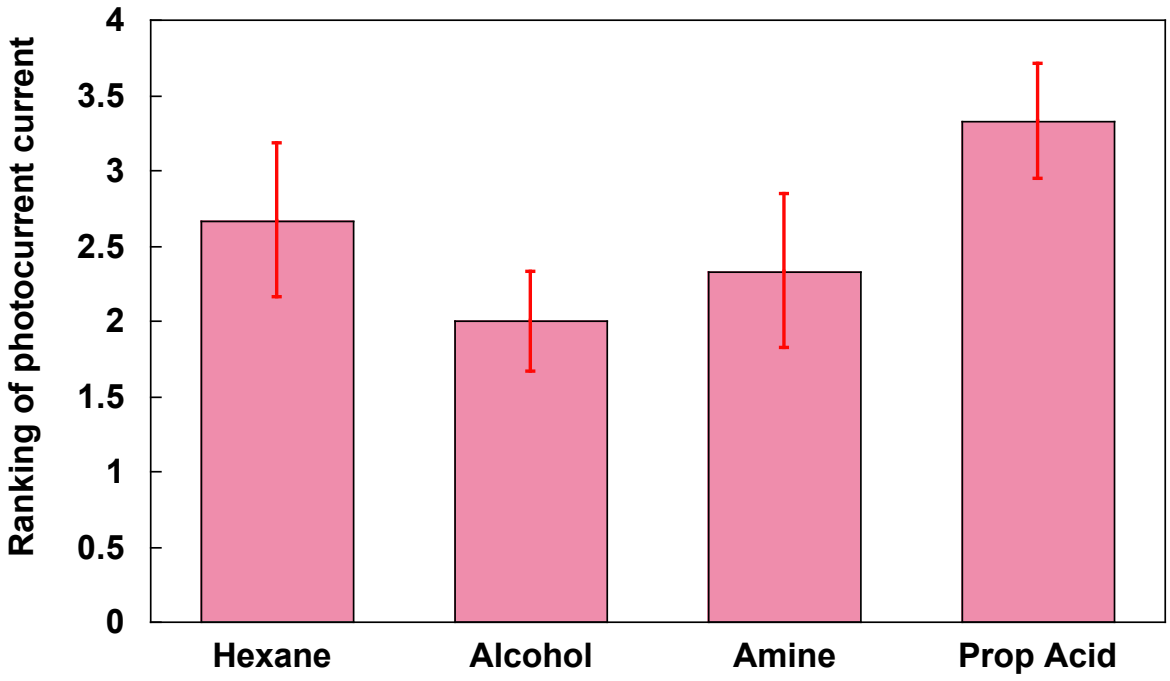

Figure A- 7. Photocurrent ranking of PSI films immobilized on p-Si with different functional groups

Then organic chemicals with different number of carbons have been assembled onto p-Si. The photocurrent of PSI multilayer films immobilizing on these substrates was tested again. It showed PSI films generated photocurrent in similar magnitude while the PSI immobilizing on etched Si had a much higher current (Figure A-8). The stability of photocurrent measurement has also been performed. A photocurrent measurement was taken 30 min after the initial test (Figure A-9)., and Figure A-10 shows the photocurrent remaining after 30 min, indicating that the photocurrent remaining of PSI films immobilized on organic monolayer films was 60%~70%. However, for the PSI films immobilized on etched Si, its photocurrent remaining was less than 5% after 30 min, which was much lower than the surfaces protected by monolayers. This result is attributed to the fact that the organic monolayer could protect the

surface by blocking the air. At the same time, though, the organic film is very thin, but sit still hinder initial performance of PSI film.

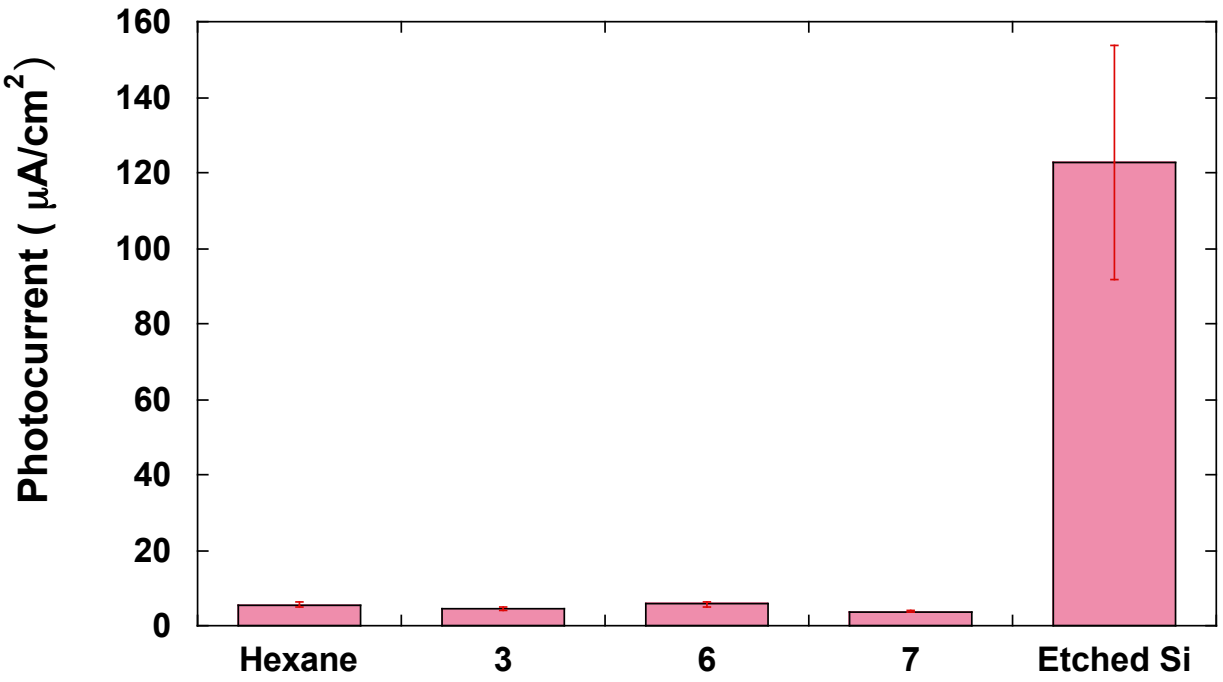

Figure A- 8. Photocurrent of PSI films immobilizing on different monolayers on p-Si

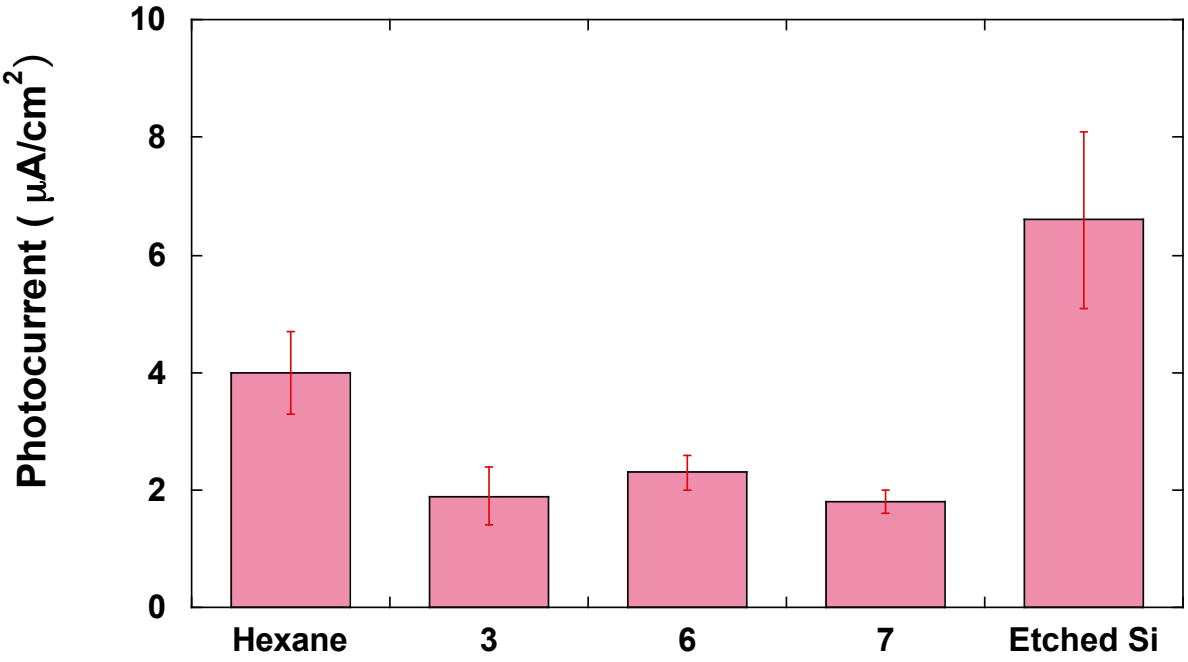

Figure A- 9. Photocurrent of PSI films immobilizing on different monolayers on p-Si after 30 min exposure to ambient air.

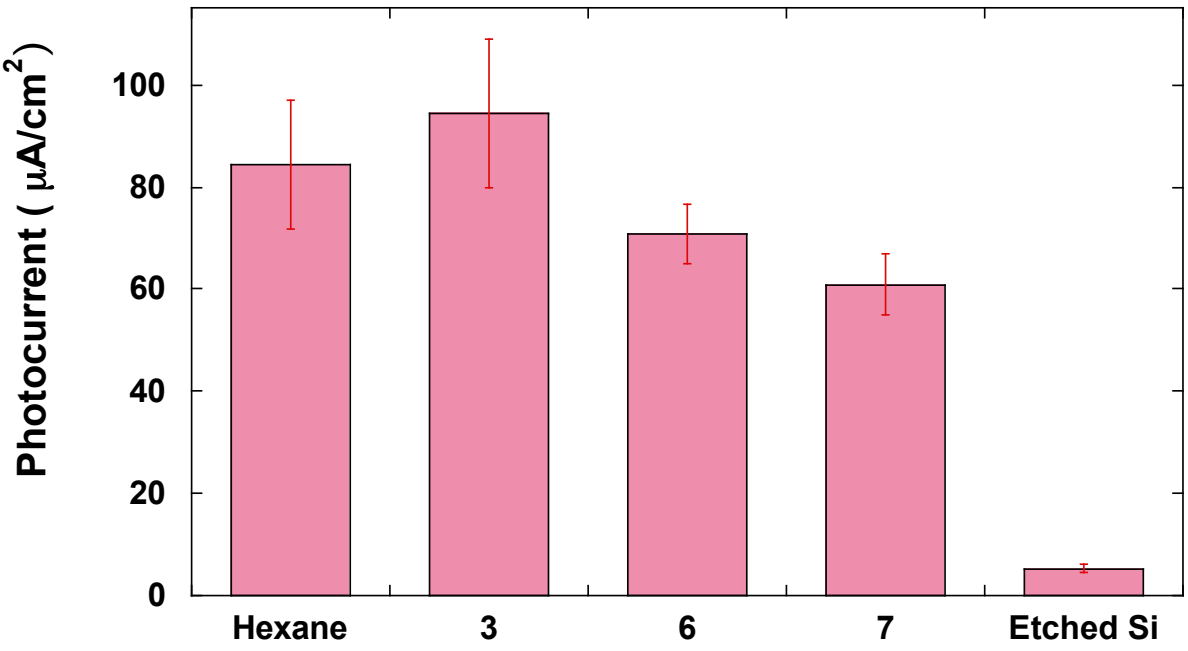

Figure A- 10. Percentage of photocurrent remaining of PSI films immobilized on different monolayers on p-Si after 30 min

The Stability of PSI Multilayer Films under Different Temperatures

With the same methods discussed before, PSI multilayer films on gold were prepared by the vacuum-assisted method. The films were heated to various temperatures from 20℃ to 80℃ for 10 min. After heating, photocurrent measurement was taken to characterize the PSI films. Steady state photocurrent was obtained from the measurement and shown in Table A-4. It showed that photocurrent decreased to 0 at 80℃ as the protein lost its activity. Photocurrent obtained from different temperatures did not have a straightforward trend; it could be that 10 min heating exposure may not be long enough to damage the protein through to different extents.

Table A- 4. Photocurrent results of PSI films heated at various temperatures

Temperature(°C)	Steady State Current Density (μA/cm2)
20	5.5
40	3.9
50	4
60	4.9
70	4.9
80	-0.1

To future test the stability of PSI films exposed to different temperatures, we have obtained the photocurrent of PSI films exposed to 50℃ and 70℃ for 4 h respectively. The photocurrent remained at 50℃ very well for a longer time while the photocurrent decreased markedly at 70℃, suggesting that the protein is deactivated upon exposure to the higher temperature.

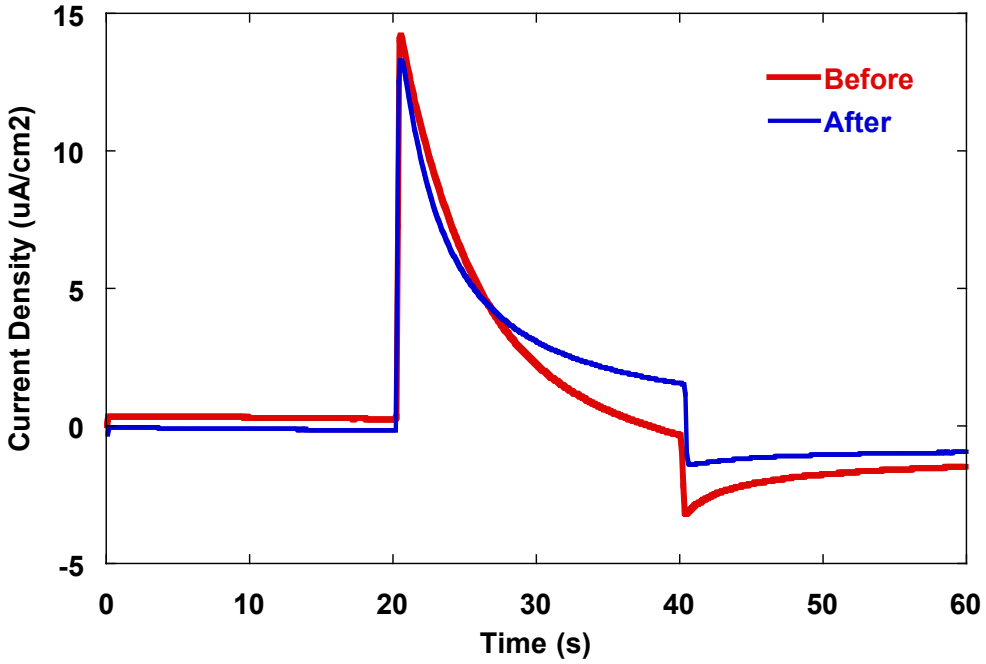

Figure A- 11. Photocurrent of PSI films exposed to 50℃ in air for 4 h

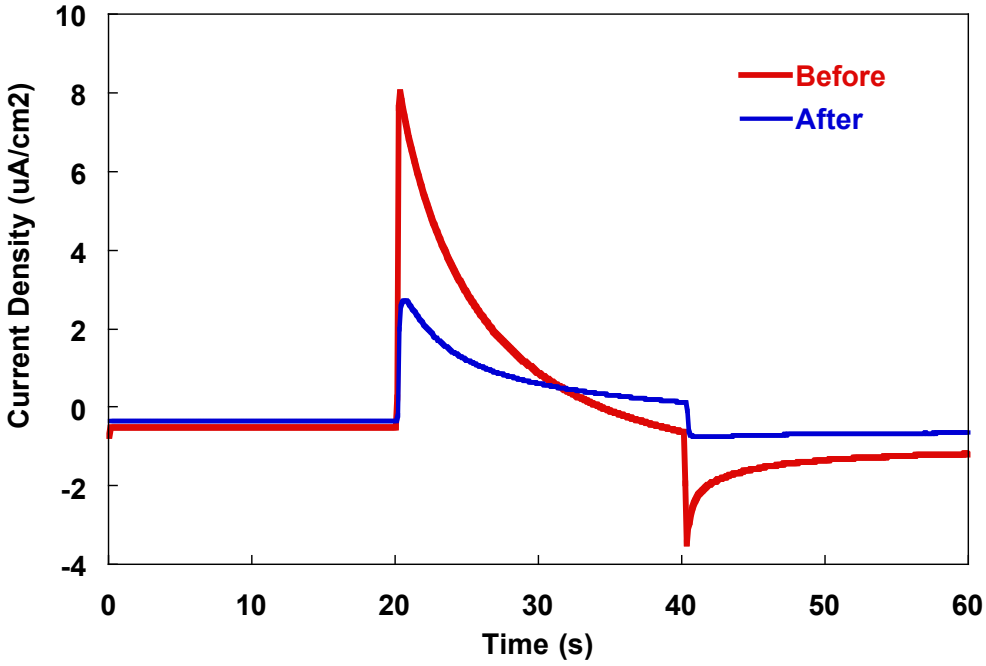

Figure A- 12. Photocurrent of PSI films exposed to 70℃ in air for 4 h